

# Helicity dynamics, inverse and bi-directional cascades in fluid and magnetohydrodynamic turbulence: A brief review

A. Pouquet<sup>1,2</sup>, D. Rosenberg<sup>3</sup>, J.E. Stawarz<sup>4</sup> and R. Marino<sup>5</sup>

<sup>1</sup>Laboratory for Atmospheric and Space Physics, Boulder, CO 80309 USA.

<sup>2</sup>NCAR, P.O. Box 3000, Boulder, CO 80307 USA.

<sup>3</sup>NOAA, Boulder, CO, United States.

<sup>4</sup>Department of Physics, Imperial College London, United Kingdom.

<sup>5</sup>Laboratoire de Mécanique des Fluides et d'Acoustique, CNRS, École Centrale de Lyon, Université de Lyon, INSA de Lyon-1, F-69134 Écully, France

## Key Points:

- Magnetic helicity displays an inverse cascade to large scales which, in electron MHD, can be justified with a simple phenomenological model
- Total energy in MHD or rotating stratified turbulence has constant-flux cascades to small and large scales, affecting mixing and dissipation
- With these results, needed modifications to sub-grid scale turbulence models will be enhanced using tools from big-data and machine-learning
- 
- 
- Published on line, *Earth and Space Science*, AGU/Wiley, March 6, 2019.
- Special Section: Nonlinear Systems in Geophysics: Past Accomplishments and Future Challenges
- DOI:10.1029/2018EA000432.
- 

arXiv:1807.03239v2 [physics.flu-dyn] 12 Mar 2019

**Abstract**

We review helicity dynamics, inverse and bi-directional cascades in fluid and magnetohydrodynamic (MHD) turbulence, with an emphasis on the latter. The energy of a turbulent system, an invariant in the non-dissipative case, is transferred to small scales through nonlinear mode coupling. Fifty years ago, it was realized that, for a two-dimensional fluid, energy cascades instead to larger scales, and so does magnetic excitation in MHD. However, evidence obtained recently indicates that in fact, for a range of governing parameters, there are systems for which their ideal invariants can be transferred, with constant fluxes, to both the large scales and the small scales, as for MHD or rotating stratified flows, in the latter case including with quasi-geostrophic forcing. Such bi-directional, split, cascades directly affect the rate at which mixing and dissipation occur in these flows in which nonlinear eddies interact with fast waves with anisotropic dispersion laws, due for example to imposed rotation, stratification or uniform magnetic fields. The directions of cascades can be obtained in some cases through the use of phenomenological arguments, one of which we derive here following classical lines in the case of the inverse magnetic helicity cascade in electron MHD. With more highly-resolved data sets stemming from large laboratory experiments, high-performance computing and *in-situ* satellite observations, machine-learning tools are bringing novel perspectives to turbulence research. Such algorithms help devise new explicit sub-grid scale parameterizations, which in turn may lead to enhanced physical insight, including in the future in the case of these new bi-directional cascades.

**Plain-language Summary** Turbulent flows are ubiquitous in Geophysics and Space Physics. They are complex, involving interactions between eddies and waves at widely separated scales, with the energy flowing in the general case only to small scales to be dissipated. It was found recently that, contrary to such expectations, energy can go in substantial amounts to both the small scales and to the large scales, in the presence of magnetic fields, as applicable to space plasmas as in the Solar Wind, and for rotating stratified flows as encountered in the atmosphere and the oceans. This result implies that the amount of energy available for dissipation may differ from flow to flow and simple scaling arguments allow for predictions that are backed up by results stemming from direct numerical simulations. One should incorporate this bi-directional cascade phenomenon in the turbulence models used for global computations of geophysical and astrophysical media. In fact, machine-learning tools may prove useful in deriving such enhanced models in their capacity to interrogate the large numerical, observational and experimental data bases that already exist for such complex flows, with the potential to lead to a deeper understanding and to more accurate predictions of such flows.

**1 Introduction**

Turbulence prevails in many geophysical and astrophysical flows, and progress is being made presently in the understanding of such flows for fluids, neutral or conducting, including in the presence of waves stemming from strong rotation, stratification, compressibility or quasi-uniform magnetic fields. The complexity of turbulent flows comes from the nonlinearity of the underlying equations leading to multi-scale interactions through mode coupling. It can result in a non-universality of spectra in models of magnetohydrodynamic (MHD) turbulence (Beresniak, 2014; Lee, Brachet, Pouquet, Mininni, & Rosenberg, 2010; P. D. Mininni & Pouquet, 2007; Perez, Mason, Boldyrev, & Cattaneo, 2014), with applications to Solar Wind dynamics (Galtier, 2012) or laboratory plasmas (Bratanov, Jenko, Hatch, & Wilczek, 2013). It is also at the source of a wide variety of behavior, from the appearance at small scales of sharp structures such as tornadoes, to large-scale pattern formation, coherent vortices and jets. This type of ordered motion at large scale is not limited to physical systems. For example, large-scale structures are also encountered in micro-biology in the context

of the collective behavior of constituents within so-called active fluids (see Reinken, Klapp, Bär, and Heidenreich (2018) and references therein, in a fast-moving domain of research), involving interactions between the solvent (say, water) and self-propelled micro-organisms such as bacteria (Dombrowski, Cisneros, Chatkaew, Goldstein, & Kessler, 2004; Wensink et al., 2012). By collective behavior, it is meant the dynamics of a group viewed as an entity, a phenomenon that can be encountered in statistical physics, for example for the Ising model, as well as in other fields such as voter or crowd dynamics (Castellano, Fortunato, & Loreto, 2009).

Substantial advances in the understanding of nonlinear systems have dealt with the zero-dimensional case in which temporal chaos in an otherwise spatially ordered field is observed in many instances, together with fractal behavior, leading to remarkable scaling laws (see several reviews in this Special Issue). Similarly, in one spatial dimension, solitons can arise through an exact balance between dispersion and nonlinear steepening, due for example to advection, as in the Korteweg-de-Vries or Kuramoto-Sivashinsky equations. Finally, in higher spatial dimensions, the seminal discovery, first for two-dimensional neutral fluids (Kraichnan, 1967) of the possibility of an inverse cascade has led to a fundamentally different view of turbulent flows beyond the venue that mode-coupling offers for energy dissipation in the small scales. Inverse cascades are defined here as an excitation reaching scales larger than the forcing scale because of constraints due to the presence of more than one ideal quadratic invariant in the non-dissipative case.

Inverse and direct cascades are found in other systems, such as nonlinear optics. For example in Newell and Zakharov (2008), a direct connection to dissipation at small scales through instabilities of coherent structures at large scales is stressed in such a context. Indeed, in the presence of an inverse cascade leading to instabilities of these large-scale coherent structures, one prediction of weak turbulence – that is, turbulence with waves that are faster than nonlinear eddies – is that there is stronger intermittency in the small scales. This enhanced intermittency can be linked to the presence of strong and sporadic small-scale structures such as vortex and density filaments in the interstellar medium, and current sheets in the Earth’s magnetosphere. It should be noted that the corrections to simple (dimensional) scaling laws for turbulent fluids can be computed analytically in some cases, such as for the passive scalar (Kraichnan, 1994), and progress is being made using non-perturbative renormalization group theory for fully developed turbulence (FDT) (Canet, Delamotte, & Wschebor, 2016). Moreover, in weak MHD turbulence in the presence of a strong uniform magnetic field, small-scale intermittency is found as well, together with nonlocal coupling of scales (Meyrand, Kiyani, & Galtier, 2015). In weak Langmuir turbulence, such a coupling between large-scale coherent structures, formed by an inverse cascade in the form of Langmuir cavitons, and strong small-scale turbulence, is also advocated in the coupling of these two forms of turbulence (Henri, Califano, Briand, & Mangeney, 2011). Similarly, the non-Gaussian wings observed for example in four-wave interactions for Langmuir waves are associated with wave breaking, and intermittency is stronger when the linear and nonlinear characteristic times become comparable (Choi, Lvov, Nazarenko, & Pokorni, 2005). A simple case of such a strong intermittency, when linear and nonlinear characteristic times are comparable, is that of the vertical velocity of rotating stratified flows; a model for it can be developed for a Philipps saturation spectrum (Dewan, 1997), as shown for example in recent direct numerical simulations (DNS) (Feraco et al., 2018; Rorai, Mininni, & Pouquet, 2014), or when the shorter time-scale of the problem is that associated with random sweeping (Clark di Leoni, Cobelli, & Mininni, 2015).

These new results are due to a combination of technological, observational, numerical and theoretical advances, with the help of several large-scale laboratory experiments such as the Coriolis table to study rapidly rotating turbulence, in the presence

or absence of stratification (Aubourg et al., 2017). Similarly, high values of the control parameter, namely the Reynolds number which measures the relative strength of nonlinearities to (linear) dissipation, are achieved nowadays using liquid helium (Saint-Michel et al., 2014). At the same time, a multitude of observations are increasing our understanding of such complex fluids, with various space missions (Marino et al., 2008, 2011; Tsurutani et al., 2016), now including using data stemming from MMS (Magnetospheric Multi-Scale, see *e.g.* Burch et al. (2016)), looking at turbulence in the magnetotail (Ergun et al., 2018) or in the magnetosheath (Gershman et al., 2018), as well as in the Solar Wind in general (Chasapis et al., 2017).

Such studies of the Earth’s plasma environment can lead to advance warnings of strong solar eruptions and their ensuing disruption on satellite communications (Casak et al., 2017). In parallel, progress in high-performance computing is allowing for numerical simulations at Reynolds numbers that were not explored before with sufficient accuracy in the absence of modeling terms (de Bruyn Kops, 2015; Ishihara, Morishita, Yokokawa, Uno, & Kaneda, 2016; Iyer, Sreenivasan, & Yeung, 2017; Rosenberg, Pouquet, Marino, & Mininni, 2015; Zhai & Yeung, 2018). And a renewal of interest in the theory of weak turbulence has allowed for the exploration of small-scale and large-scale intermittency as diagnosed in the occurrence of extreme events, such as fronts and filaments in the ocean (McWilliams, 2016), or current sheets in MHD (P. Mininni, Pouquet, & Montgomery, 2006; Zhou, Matthaeus, & Dmitruk, 2004), as well as shocks in compressible flows (Porter, Pouquet, & Woodward, 2002), all events making such flows largely unpredictable. A picture of turbulence is thus emerging that broadens our understanding which, in some instances, dates back to the mid forties for homogeneous isotropic turbulence, for example concerning the possible scaling laws for energy spectra, classically compared to the Kolmogorov (1941) law for the kinetic energy spectrum, namely  $E_V(k) \sim \epsilon_V^{2/3} k^{-5/3}$ , where  $k$  is the isotropic wavenumber and  $\epsilon_V$  the kinetic energy dissipation rate. It is in this context that we now review results on helicity, and on inverse and bi-directional cascades in MHD and fluid turbulence, with an emphasis on the former.

## 2 The role of kinetic helicity

We first recall the general properties of kinetic helicity,  $H_V$ , in fluid turbulence. It is defined as the space-integrated correlation between the velocity field  $\mathbf{u}$  and the vorticity  $\boldsymbol{\omega} = \nabla \times \mathbf{u}$ , and is an invariant of the ideal equations of motion for FDT, as well as for purely rotating flows. Helicity is not definite positive: it can be of either sign, representing a (partial) alignment or anti-alignment of velocity and vorticity. Helicity has been studied extensively in the laboratory and in numerical simulations (Biferale, Musacchio, & Toschi, 2012; Moffatt & Tsinober, 1992); it is strong in vortex filaments in FDT (Kerr, 1985, 1987), as well as in quantum turbulence (Clark di Leoni, Mininni, & Brachet, 2017). It has recently been detected in DNS using helicoid particles (Gustavsson & Biferale, 2016), particles which are sensitive to the lack of mirror symmetry of the flow in which they are embedded. The decay of energy is considerably slowed down in the presence of strong helicity for either rotating turbulence (Teitelbaum & Mininni, 2011), or in the stratified case (Rorai, Rosenberg, Pouquet, & Mininni, 2013). The helicity spectrum has been observed in the Planetary Boundary Layer (Koprov, Koprov, Ponomarev, & Chkhetiani, 2005); it is found to be rather flat when the stable stratification is strong, a finding also present in DNS (Rorai et al., 2013). Helical modes have also been identified in secondary instabilities in boundary layer flows leading to the formation of turbulent spots (Bose & Durbin, 2016).

In Hurricane Bonnie (1998), velocities, helicity and brightness temperature were monitored with tropospheric drop sondes (Molinari & Vollaro, 2008, 2010). Hurricanes are associated with strong helicity since, outside the boundary layer, they can be viewed as a quasi two-dimensional rotating stratified flow, thus with mostly vertical

vorticity, together with a strong updraft or downdraft. Apart from the atmosphere, helicity in geophysical flows is observed in secondary currents in river bends and confluences. It affects the salt distribution in estuaries, interactions with tidal flows, and at river confluences, the transport of sediments and mixing, erosion, and morphology (Constantinescu, Miyawaki, Rhoads, Sukhodolov, & Kirkil, 2011). Furthermore, stratification is seen as playing an essential role in the formation and structure of submarine turbidity currents, as measured and analyzed in Azpiroz-Zabala et al. (2017), leading to sediment suspension and transport for long distances. Helicity is produced by hydrostatic and geostrophic balance between the Coriolis force, gravity and pressure gradients, while neglecting the nonlinear advection term (Hide, 2002; Marino, Mininni, Rosenberg, & Pouquet, 2013). In tropical storms, helicity is associated with the presence of coherent structures in the form of roll vortices in the boundary layer of typhoons, structures which are linked with inflection-point shear instabilities (Morrison, Businger, Marks, Dodge, & Businger, 2005). Similarly, at river confluences, large-scale turbulence structures are produced in the form of stream-wise oriented helical vortical eddies. When such structures are observed, the mixing properties downstream of the confluence and the mixing interface between the two volumes of water, sometimes of quite different turbidity and salinity, are altered. Helical structures also interact with shear layers, leading to the formation of turbulent motions (Constantinescu et al., 2011). Moreover, helicity can lead to large-scale instabilities (Frisch, She, & Sulem, 1987; Levina & Montgomery, 2014; Yokoi & Brandenburg, 2016), and it has been shown to slow-down the temporal evolution of shear flows as well, necessitating a change in the modeling formalism of the unresolved small scales, by incorporating turbulent transport coefficients that are helicity-dependent (Baerenzung, Mininni, Pouquet, & Rosenberg, 2011; Baerenzung, Politano, Ponty, & Pouquet, 2008; Yokoi & Yoshizawa, 1993). The role of helicity in sub-grid scale models has also been analyzed recently, numerically as well as analytically, in the latter case using upper bounds on weak solutions of the Navier-Stokes equations (Linkmann, 2018).

One can define spectral densities of energy and helicity in terms of isotropic wavenumber  $k$ ,  $[E_V(k), H_V(k)]$ , and with  $\langle \mathbf{u} \cdot \mathbf{u} \rangle = 2 \int E_V(k) dk$ ,  $\langle \mathbf{u} \cdot \boldsymbol{\omega} \rangle = 2 \int H_V(k) dk$  the total kinetic energy and helicity, angular brackets standing for volume integration. With such definitions, one has  $-1 \leq \sigma_V(k) = H_V(k)/[kE_V(k)] \leq 1$  for the so-called relative helicity density  $\sigma_V(k)$ , using a Cauchy-Schwarz inequality. In FDT, both  $E_V(k)$  and  $H_V(k)$  follow a  $k^{-5/3}$  spectral law and thus the return to isotropy in homogeneous isotropic turbulence, with full recovery of mirror symmetry ( $\sigma_V(k) \rightarrow 0$ ), occurs at a rate proportional to  $1/k$  as  $k \rightarrow \infty$ . Note that isotropy here is meant solely as an invariance to rotation, but lack of mirror reflections is allowed, as measured by non-zero velocity-vorticity correlations.

The analysis of triad interactions decomposed into two circularly polarized ( $\pm$ ) helical modes as done in Waleffe (1992) shows that an inverse transfer of energy to larger scales takes place when the two small-scale modes of a given triad have the same helical polarity. Although overall the energy cascade is to the small scales, as predicted in Kraichnan (1973), this feature was exploited in Biferale et al. (2012) by restricting interactions to one-signed helical modes and observing numerically an inverse cascade of energy in that truncated case. This result further led to the derivation of global regularity in these truncated systems (Biferale & Titi, 2013). Such a helical decomposition is rather common; it has been used in so-called shell models (Lessines, Plunian, & Carati, 2009), or in the context of the dynamo problem (Linkmann, Sahoo, McKay, Berera, & Biferale, 2017).

A further and rather intriguing result, as analyzed in Alexakis (2017), is that in fact, the total energy flux can be decomposed into three different sub-fluxes that are individually constant in the inertial range, hinting at some, as yet undetermined, invariants and, as pointed out in the paper, leading to additional exact laws in terms

of third-order structure functions. Similarly, the helicity flux can be partitioned into two independently constant partial fluxes, indicative that the behavior of such flows is more constrained than thought previously. It is not clear whether this corresponds to the separate invariance of the (two) energies of these modes. Similarly, for MHD turbulence, the invariance of total energy and cross helicity, namely  $E_T = E_V + E_M$  and  $H_C = \langle \mathbf{u} \cdot \mathbf{b} \rangle$ , can be expressed as two definite-positive invariants, in the ideal, non-dissipative case, in terms now of the so-called Elsässer variables  $\mathbf{z}_{\pm} = \mathbf{u} \pm \mathbf{b}$ , of energies  $E_{\pm}$ . So the question arises as to whether there are also in MHD sub-fluxes that are independently constant in the inertial range, a point open for future research.

Recently, it was also shown in Słomka and Dunkel (2017) that, in the context of bacterial suspensions and using the Navier-Stokes equations for the solvent with a stress tensor including higher-order terms modeling the role of the non-Newtonian active part of the fluid, an accumulation of energy at large scales occurred because of an instability due to the bi-Laplacian forcing. One peculiar feature of these solutions is that they can be fully helical, Beltrami flows,  $\boldsymbol{\omega} = \lambda \mathbf{v}$  by selecting the scales for which the three linear terms (proportional in Fourier space to  $k^{2n}$ ,  $n = 1, 2, 3$ ) can balance each other exactly. Note that this corresponds to a viscous-forcing-dissipation balance, somewhat similar to the large-scale quasi-geostrophic equilibrium in rotating stratified flows involving, rather, dispersive effect of inertia-gravity waves and the pressure gradient. Such an inverse energy cascade occurs through spontaneous mirror-symmetry breaking as being the cause of the selection of triadic interactions. Indeed, these new terms in the stress tensor can induce, when the equation is linearized, instabilities of the large scales because of a limited range of unstable Fourier modes depending on the governing parameters.

### 3 Coupling to a magnetic field

#### 3.1 Dynamical equations and parameters

For completeness, one can write the MHD equations in the incompressible case (see, *e.g.*, Davidson (2013); Galtier (2016); Pouquet (1993, 1996)), including the Hall current added to a (generalized) Ohm's law. The Hall MHD (HMHD) equations are:

$$\frac{\partial \mathbf{v}}{\partial t} = -\mathbf{v} \cdot \nabla \mathbf{v} - \nabla P + \mathbf{J} \times \mathbf{B} + \nu \nabla^2 \mathbf{v} - \nu' \nabla^4 \mathbf{v} \quad (1)$$

$$\frac{\partial \mathbf{B}}{\partial t} = \nabla \times (\mathbf{v} \times \mathbf{B}) - \epsilon_H \nabla \times (\mathbf{J} \times \mathbf{B}) + \eta \nabla^2 \mathbf{B} - \eta' \nabla^4 \mathbf{B}, \quad (2)$$

together with  $\nabla \cdot \mathbf{v} = 0$ ,  $\nabla \cdot \mathbf{B} = 0$ . The magnetic field is expressed in Alfvén velocity units,  $P$  is the pressure, and  $\mathbf{J} = \nabla \times \mathbf{B}$  the current density;  $\nu$  and  $\eta$  are the kinematic viscosity and magnetic diffusivity, and  $\nu'$ ,  $\eta'$  are hyperviscosity and hyperdiffusivity coefficients associated with bi-Laplacian terms. Their respective roles on the formation of small-scale current sheets are discussed in detail in J. E. Stawarz and Pouquet (2015) (see also Figure 1, for which we took  $\nu = \eta$ ,  $\nu' = 0 = \eta'$ .)

The Reynolds, Froude and Rossby numbers are defined as  $Re = U_0 L_0 / \nu$ ,  $Fr = U_0 / [NL_0]$  and  $Ro = U_0 / [fL_0]$ , with  $U_0, L_0$  being characteristic velocities and length scales based on the computed *rms* velocity and integral length scale. They measure the strength of nonlinearities relative to dissipation, stratification or rotation respectively, with  $f = 2\Omega$ ,  $\Omega$  being the rotation assumed to be in the vertical ( $z$ ) direction. The buoyancy Reynolds number is  $\mathcal{R}_B = ReFr^2$ . The magnetic Reynolds number is  $R_M = U_0 L_0 / \eta$  and  $P_M = \nu / \eta$  is the magnetic Prandtl number. The dimensionless parameter  $\epsilon_H = d_i / L_0$  giving the ratio of the ion inertial length to the integral length scale of the system characterizes the strength of the Hall current. When  $\epsilon_H = 0$ , the HMHD equations reduce to the MHD equations, and the Navier-Stokes equations are obtained by further setting  $\mathbf{B} = 0$ . The electron-MHD equations are written separately in §3.4.



### 3.2 The direct cascade of energy to small scales

In three-dimensional MHD, the ideal invariants in the absence of dissipation are the total energy  $E_T = E_V + E_M = 1/2 \langle |\mathbf{u}|^2 + |\mathbf{B}|^2 \rangle$ , the magnetic helicity  $H_M = \langle \mathbf{A} \cdot \mathbf{B} \rangle$  with  $\mathbf{B} = \nabla \times \mathbf{A}$  (where  $\mathbf{A}$  is the magnetic vector potential), and the cross-correlation between the velocity and magnetic field,  $H_C = \langle \mathbf{u} \cdot \mathbf{B} \rangle$  (Blackman, 2015; Pouquet, 1996; Woltjer, 1960). The total energy cascades to small scales, both in two and in three dimensions, with a self-similar spectrum whose spectral index might still be in dispute (Beresniak, 2014; Lee et al., 2010; P. D. Mininni & Pouquet, 2007; Perez et al., 2014), a matter that is rendered difficult (i) by the anisotropy of such flows especially in the small scales because of the presence of a uniform (or quasi-uniform) strong magnetic field in the large scales; (ii) by the presence of non-zero correlations between the velocity and the magnetic field, as well as (iii) by intermittency effects leading to the steepening of these spectra. Indeed, the intermittency in MHD is known to be stronger than for FDT, and to be variable as well. For example, the anomalous exponents for the scaling of structure functions depend on the intensity of solar flares (Abramenko & Yurchyshyn, 2010). Energy spectra have been observed in the Solar Wind consistently over the years (see *e.g.* Marino et al. (2008); Matthaeus and Goldstein (1982); Veltri, Carbone, Lepreti, and Nigro (2009)). They correspond to a direct energy cascade which leads to plasma heating (Marino et al., 2011; J. Stawarz, Smith, Vasquez, Forman, & MacBride, 2009), potentially through reconnection events of current and vorticity sheets, as recently detected for example in the Earth's magnetosheath (Phan et al., 2018). However, there are a variety of possible mechanisms for the dissipation of turbulence in collisionless space plasmas, such as current driven instabilities (J. E. Stawarz, Ergun, & Goodrich, 2015), and it is still an open question as to what the dominant mechanisms are. Reconnection is also present in numerous numerical studies (see *e.g.* Higashimori, Yokoi, and Hoshino (2013); Karimabadi et al. (2013); Loureiro, Schekochihin, and Uzdensky (2013); P. Mininni et al. (2006); Ting, Matthaeus, and Montgomery (1986); Zhou et al. (2004)), and in plasma relaxation processes (Taylor, 1986). Finally, there are recent indications, using small-scale laboratory experiments, that the source of the turbulence may not matter in the resulting spectral dynamics of such MHD flows (Chatterjee et al., 2017).

The observation of magnetic fields in planets and stars, in the interstellar medium or in galaxies leads to the question of their origin. Many review papers and books have been devoted to this topic, and one can consult for example Brandenburg and Subramanian (2005); Galtier (2016); Pouquet (1993, 1996). They may be primordial remnants from the early universe, or they may arise from a generation mechanism from a seed field  $\mathbf{b}$  coupled to the velocity, through what is called the dynamo effect. Reversals of the geomagnetic field occur in a rather reproducible way, on average, with fast growth and slower decay phases that are comparable between different geological periods (Valet & Fournier, 2016). It has been known, since Parker's model and the mean field theory developed in Steenbeck, Krause, and Rädler (1966), that helicity is an essential ingredient of such a dynamo mechanism for creating large-scale fields. Note however that one can find examples of non-helical dynamos that can take place through chaotic stretching of magnetic field lines (see *e.g.* Childress and Gilbert (1995); Nore, Brachet, Politano, and Pouquet (1997); Ponty, Pouquet, and Sulem (1995)). Once a strong magnetic field is generated, it leads to wave propagation and to a weak turbulence regime that has been detected in the magnetosphere of Jupiter (Saur, Politano, Pouquet, & Matthaeus, 2002). It also leads to the development of localized vorticity and current sheets which further roll-up as the turbulence increases for sufficiently high Reynolds numbers (Lee et al., 2010), as observed for example in the Earth's magnetosphere (Alexandrova et al., 2006; Osman et al., 2014).

The decay of energy is lessened in the presence of cross-helicity, *i.e.* the correlations between the velocity and the magnetic field (Marino et al., 2012; Pouquet, Sulem,

& Meneguzzi, 1988; Smith, Stawarz, Vasquez, Forman, & MacBride, 2009). This corresponds again to an alignment, here of the velocity and the magnetic field, which weakens the nonlinear terms, directly for Ohm's law, and indirectly for the Lamb vector  $\mathbf{u} \times \boldsymbol{\omega}$  which can be compensated exactly, when the correlations are strong, by the Lorentz force  $\mathbf{B} \times \mathbf{j}$ . The role of symmetries in the long-time evolution of MHD flows, using an energy minimization principle, has been shown to lead to final states governed by the relative magnitude of ideal invariants (J. Stawarz, Pouquet, & Brachet, 2012; Stribling & Matthaeus, 1990, 1991). Furthermore, the role of anisotropy is central in the dynamics of the cross-correlation, as shown in Briard and Gomez (2018) using a two-point closure of MHD turbulence, and it should be investigated further. It is known that the return to isotropy in the small scales can be slow, as for example in the presence of rotation (P. Mininni, Rosenberg, & Pouquet, 2012). Recent laboratory experiments (Baker, Poth erat, Davoust, & Debray, 2018) and high-resolution numerical simulations on grids of up to  $16384 \times 2048^2$  points (Zhai & Yeung, 2018), have studied MHD anisotropy and its relationship with dual cascades. It is found that 2D and 3D coherent structures, in the bulk and at the wall, can cohabit. In fact, such a transition also exist in variations of the Navier-Stokes equations having the same inviscid invariants (energy and helicity) and the same symmetries (under rotation, reflection and scaling). It can be analyzed in terms of critical point behavior with divergence of the fluctuations field at the transition (Sahoo, Bonaccorso, & Biferale, 2017).

### 3.3 Inverse cascade of magnetic helicity

Magnetic helicity is observed in the solar photosphere (see *e.g.* Blackman (2015) and references therein), and in the Solar Wind (Howes & Quataert, 2010). Its dynamical role in coronal mass ejections can be modeled through the twisting and reconnection of magnetic flux tubes (Gibson & Fan, 2008; Malapaka & M uller, 2013), and it is known to undergo an inverse cascade to large scales (Frisch, Pouquet, L eorat, & Mazure, 1975; Pouquet, 1993, 1996; Pouquet, Frisch, & L eorat, 1976).

In Figure 1, we give the temporal development in MHD of the magnetic energy and helicity spectra,  $H_M(k)$ ,  $E_M(k)$  (top left and right), and the kinetic energy spectra,  $E_V(k)$ , bottom left. Forcing is for  $k_F \approx 20$ ; times are given in the inset in units of the turnover time  $\tau_{NL} = L_0/U_0$ . The Geophysical High-Order Suite for Turbulence (GHOST) code is used (P. Mininni, Rosenberg, Reddy, & Pouquet, 2011) with grids of  $128^3$  points; boundary conditions are periodic, and only a normal Laplacian operator is present. One observes the progressive build-up of  $H_M$  at large scale which entrains the magnetic energy, since  $E_M(k) \geq k|H_M(k)|$ ; this build-up of  $E_M(k)$  then leads to a similar growth of kinetic energy at large scales because of the effect of Alfv en waves (Pouquet et al., 1976). The figure here is a simple illustration of the phenomenon. Detailed triadic interactions of such an inverse cascade are studied in Linkmann and Dallas (2017); Linkmann et al. (2017) using a classical helical decomposition, with both analytical and numerical tools at resolutions of  $512^3$  points. These authors show in particular that the relative signs of kinetic and magnetic helicity play a direct role in the emergence of large-scale dynamo fields, with growth-rates that are determined in the ideal (non-dissipative) case and thus independent of the magnitude of the magnetic Reynolds number, with no subsequent so-called  $\alpha$ -quenching (see also (Pouquet et al., 1976)).

We show, in the bottom right of Fig. 1, small-scale current structures drawn at the peak of dissipation in the presence of a Hall current. Here, the run is unforced, with random initial conditions, again no hyperviscosity, and it is performed on a more highly-resolved grid of  $512^3$  points. Note the strong localized structures. This is discussed further below in the context of electron MHD, which is a simplification of HMHD where one assumes that protons are stationary, an hypothesis which is potentially valid for the small scales of Hall MHD.



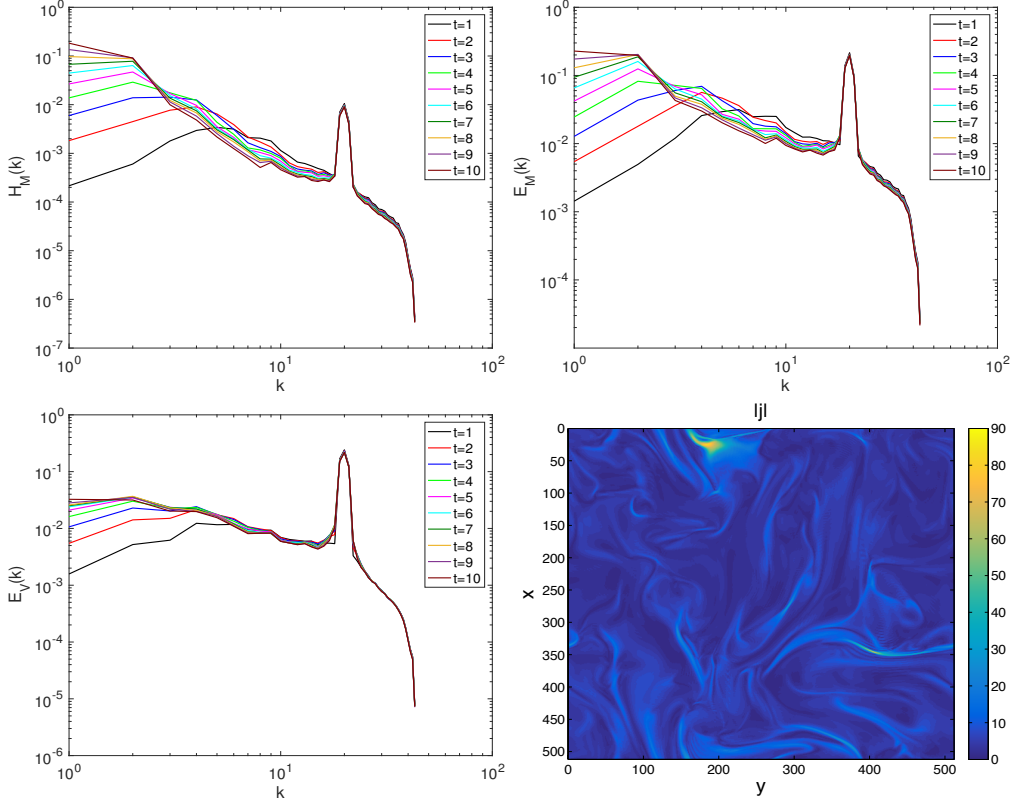


**Figure 1.** Spectra, drawn at different times (see inset), in forced MHD turbulence for magnetic helicity and energy (top left and right), and for kinetic energy (bottom left); new runs on grids of  $128^3$  points without hyperviscosity ( $\nu' = \eta' = 0$  in eqs. (1, 2)). Note the accumulation of excitation at large scale as time increases. *Bottom right:* horizontal cut for Hall-MHD of the current density for a new run on a grid of  $512^3$  points, again without hyper-diffusivities (see J. E. Stawarz and Pouquet (2015) for more detail of the general set-up).

### 3.4 Phenomenology of the inverse cascade for electron MHD

Large-scale helical structures in MHD are observed, including in the case when the forcing is non-helical, and their life-time (that is, the time spent on these states) is directly linked to the temporal correlation time of the forcing function (Dallas & Alexakis, 2015). Because such large-scale energetic structures are force-free, that is the magnetic field and current are parallel and hence the Lorentz force is zero, it poses the question of a possible linearization of turbulent flows around such stable states in plasma relaxation processes (Taylor, 1986). Magnetic helicity is also detected in the laboratory in perhaps the simplest instance of the family of models for plasmas, namely electron MHD (or EMHD) (Stenzel, Urrutia, & Rousculp, 1995). In that case, the velocity of the electrons is slaved to the electric current (while ignoring protons), and the resulting equations only involve the magnetic induction  $\mathbf{B}$ ; the equations are:

$$\frac{\partial \mathbf{B}}{\partial t} + \alpha \nabla \times [\mathbf{J} \times \mathbf{B}] = \eta \nabla^2 \mathbf{B} \quad , \quad \alpha = \frac{c}{4\pi n_e e} \quad , \quad (3)$$

with  $c$  the speed of light and  $n_e$  the electron density of charge  $e$ . In the absence of dissipation, the magnetic energy  $E_M$  and the magnetic helicity  $H_M$  are conserved, and one has  $|\sigma_M(k)| \leq 1$ , with  $\sigma_M(k) = kH_M(k)/E_M(k)$ ;  $\sigma_M = \pm 1$  corresponds to the alignment (or anti-alignment) of the vector potential and the magnetic induction.

As in MHD, waves can travel along an imposed strong magnetic field, in either direction; the so-called *unbalanced* case is when more waves travel in one direction than in the other one. Since the waves in EMHD are circularly polarized, the unbalanced case results in a non-zero magnetic helicity, and thus in an inverse cascade of  $H_M$  and direct cascade of  $E_M$ . Using direct numerical simulations of decaying EMHD in 3D, it is shown in Cho (2011) that the peak of the magnetic energy spectrum moves to larger scales; this is consistent with the fact that  $|\sigma_M(k)| \leq 1$ , and the magnetic helicity may undergo an inverse transfer as well in the forced case (see also Zhu, Yang, and Zhu (2014)). However, note that the sign of the energy flux was predicted analytically to be positive in the framework of weak turbulence for EMHD, corresponding to a direct energy cascade under the assumption that there is an infra-red (large-scale) cut-off to insure locality of Fourier interactions (Galtier & Bhattacharjee, 2003) (see also Galtier and Meyrand (2015)).

An argument for the inverse cascade can be made following what is done in Fjørtoft (1953) for two-dimensional neutral fluids, since magnetic energy and helicity are dimensionally linked, with  $|\sigma_M(k)| \leq 1$ . In order to be able to straightforwardly extend the result of Fjørtoft in that case, one needs to assume that helicity is of a given sign and that it is maximal (see *e.g.* Chen, Chen, and Eyink (2003); Slomka and Dunkel (2017); Waleffe (1992) for detailed analyses of triadic interactions in helical flows). This applies, for example, to the set-up of the inverse energy cascade found for one-sign helical flows (Biferale et al., 2012). Moreover, within the large-scale helical range, the helicity is likely to be of one sign only, and in MHD at least it is known to be maximal in the largest scales, corresponding to force-free field configurations (Pouquet et al., 1976). It can also be noted that a mechanism for having one-sign magnetic helicity in EMHD at large scale was discussed in Zhu et al. (2014): the argument consists in remarking that, in terms of helical variables, the statistical equilibria are large-scale dominated close to their Fourier-space pole.

For the EMHD system, let us assume that we have an exchange of magnetic energy and of magnetic helicity for the triplet of wavenumbers  $[k, p = 1.5k, q = 2.25k]$  (which, for integer wavenumbers, can be the triad  $[k = 4, p = 6, q = 9]$ ); this exchange is written as  $\delta E_{M, k p q}$  and  $\delta H_{M, k p q}$ , and say that helicity is one-signed, positive, and maximal,  $H_M(k) = E_M(k)/k$ . The double constraint of conservation of total  $E_M$  and  $H_M$  leads to algebraic relations for the energy and helicity interactions between these

three wavenumbers. Thus, one obtains:

$$\delta H_{M,k} + \delta H_{M,p} + \delta H_{M,q} = 0, \quad (4)$$

$$\delta E_{M,k} + \delta E_{M,p} + \delta E_{M,q} = 0 = k\delta H_{M,k} + p\delta H_{M,p} + q\delta H_{M,q}, \quad (5)$$

due to the detailed conservation properties within each triadic interactions. In the specific case chosen here, this gives  $\delta H_{M,k} = \frac{3}{2}\delta H_{M,q}$ ,  $\delta E_{M,k} = \frac{2}{3}\delta E_{M,q}$ . So we conclude that, under these hypotheses, and starting from an excitation at the intermediate scale  $\sim 2\pi/p$ , there is more magnetic *helicity* transfer to the large scales  $\sim 2\pi/k$ , and more magnetic *energy* transfer to the small scales  $\sim 2\pi/q$ . This agrees with the fact that, in the forced case, the flux of magnetic helicity is observed to build-up an inverse cascade over time (Kim & Cho, 2015). It should be noted that, when injecting energy of  $\pm$  circularly polarized EMHD waves in a system through a forcing mechanism at some scale, one necessarily injects magnetic helicity, which can thus be regarded as a direct consequence of the properties of such waves (Cho, 2011). The ratio of the  $\pm$  injection (and dissipation) rates,  $R_{emhd} = \epsilon_+/\epsilon_- = D_t E_+/D_t E_-$  appears to be the central parameter determining the fate of these flows: the inverse energy cascade is found for  $R_{emhd} \approx 1.2$ , but instead of a pure self-similar spectrum for the energy, it takes the form of an envelope (Kim & Cho, 2015).

The direction of cascades in the presence of more than one invariant is also reviewed and analyzed at length in Alexakis and Biferale (2018). A rather novel result in MHD is that in fact the magnetic helicity undergoes constant-flux cascades to both large scales and small scales (Alexakis, Mininni, & Pouquet, 2006; Müller & Malapaka, 2013). This was shown using a detailed analysis of the degree of non-locality of nonlinear interactions (see also Debliquy, Verma, and Carati (2005)). The flux of magnetic helicity is observed, somewhat remarkably, to remain of a constant sign across the forcing scale, due to the compensating effects of the change of sign of  $H_M$  and that of the flux of  $H_M$  across that scale. The nonlocal interactions in MHD are therefore able to smooth-out the process of transfer across the scales. Using Particle In Cell numerical simulations for two-dimensional plasmas including all three components of the fields, it is argued in Che, Goldstein, and Viñas (2014), in the context of Solar Wind observations (Marino et al., 2008, 2011), that a dual magnetic energy cascade is observed which is interpreted as being due to wave-wave interactions, kinetic Alfvén waves and whistler waves, which feed both the electron and ion scales due to the anisotropy of the electric and magnetic fields, although no energy fluxes are given to confirm this finding. Anisotropy plays an essential role in this mechanism since the momentum transfer is shown to occur between the perpendicular and parallel components of the magnetic field, each transferring to either larger or smaller scales. In the latter case, this occurs together with the formation of kinetic-scale micro-current structures, as recently observed Ergun et al. (2018); Phan et al. (2018).

### 3.5 The two-dimensional case in MHD

In two dimensions, the purely magnetic invariant,  $\langle A^2 \rangle$ , is positive definite. In that case, it can be demonstrated phenomenologically, and numerically as well, that the transition between a fluid-dominated to a magnetically-dominated regime in the presence of forcing is controlled by the ratio of the kinetic to magnetic energy injection rate, namely  $\mu = \epsilon_M/\epsilon_V = D_t E_M/D_t E_V$  (Seshasanayan & Alexakis, 2016). The two-dimensionality of the flow allows for large numerical resolutions, and the critical states are identified explicitly, with the divergence of a susceptibility at the critical “temperatures” (here,  $\mu$ ), and power-law scaling close to the critical points. These points are slightly different for the change of direct to inverse cascade of magnetic potential and that of kinetic energy.

Specifically, for small magnetic forcing, in this 2D case, there is an inverse cascade of kinetic energy, and the large-scale magnetic energy spectrum corresponds to

equipartition of magnetic potential modes (or  $E_M(k) \sim k^{+3}$ ). On the other hand, for strong magnetic forcing, the equipartition is observed in the large-scale kinetic energy, whereas the magnetic potential undergoes an inverse cascade, as first derived in Fyfe and Montgomery (1976) and found using two-point closure techniques for turbulence (see review in Pouquet (1996)). These differences in spectral behavior have their counterpart in configuration space, with a change in dominant structures according to the value of the critical parameter  $\mu$ , and in the amount of intermittency as measured through the exact cubic flux relationships arising from the conservation laws of energy for the two different underlying systems (Seshasanayan & Alexakis, 2016) (see Gomez, Politano, and Pouquet (2000); Politano, Carbone, and Pouquet (1998); Politano, Gomez, and Pouquet (2003) for the 3D MHD helical case). It would be of interest to compute as well high-order moments corresponding to the fat tails in the Probability Distribution Functions that are observed to quantify the multi-fractality of these systems, and its disappearance in the inverse cascade. One of the conclusions in Seshasanayan and Alexakis (2016) is that there is a range of values of  $\mu$  for which two regimes cohabit, one mostly fluid, one mostly MHD and with at the same time a flux of energy which is both positive and constant, corresponding to the direct cascade, and negative and constant corresponding to the inverse cascade. Furthermore, two-scale instabilities in both 3D and 2D using Floquet analysis are identified in Alexakis (2018). A stability diagram is built and an overlap region of the two types of instabilities in the laminar case is found; it can be linked to the turbulent bi-directional cascade phenomenon as a function of the height of the fluid.

The two-dimensional case in the absence of a third component of  $\mathbf{u}$  and  $\mathbf{B}$  is a special subset of the more general case, in the sense that it does not allow for helical (topological) invariants, since the flow is horizontal (say) and the resulting vorticity is vertical. However, when including the third component of the fields (vertical velocity and magnetic field), the helicity is non-zero *a priori*, more invariants arise (Montgomery & Turner, 1982) and this would deserve further study since this configuration also corresponds to three-dimensional MHD in the presence of a strong uniform magnetic field (see *e.g.*, Linkmann, Buzzicotti, and Biferale (2018)). Also note that the spectral index of the inverse cascade can depend on the anisotropy of the forcing for rotating stratified turbulence (Oks, Mininni, Marino, & Pouquet, 2017).

Finally, for a 2D neutral fluid, one can show that, in the presence of a mean flow (such as vortices or jets) and turbulent fluctuations, the mean momentum stress is proportional to the mean shear (Frishman, 2017). The mean flow energy is obtained from a balance between the large-scale friction and the turbulent dissipation at small scale (Frishman & Herbert, 2018).

### 3.6 The role of anisotropy

There are several issues that merit further attention. One of them concerns the development of anisotropy in such flows. An imposed uniform rotation or uniform magnetic field, or gravity, all render the flow quasi-bi-dimensional. For rotating or for stratified flows, isotropy is recovered at small scale, beyond what is called the Ozmidov or Zeman scale,  $\ell_{Oz} = [\epsilon_V/N^3]^{1/2}$ ,  $\ell_{Ze} = [\epsilon_V/f^3]^{1/2}$ , with  $N$ ,  $f = 2\Omega$  the Brunt-Väisälä frequency and twice the rotation frequency. At these scales, the characteristic times of a wave and of a turbulent eddy are comparable, with the assumption of an isotropic Kolmogorov (1941) spectrum being recovered at small scale, and that at smaller scales, nonlinear eddies are faster. On the other hand, in the case of MHD, the opposite happens and anisotropy develops as small-scales become more two-dimensional. A uniform magnetic field  $B_0$  has a strong influence on small-scale dynamics, whereas a uniform velocity can be eliminated through Galilean invariance. This represents a difference between purely fluid and MHD turbulence. The resulting anisotropic bi-directional cascade has been studied in detail, with a progressive increase of the

inverse (quasi-2D) flux as  $B_0$  increases (see also Favier, Godeferd, Cambon, Delache, and Bos (2011); Gallet and Doering (2015); Reddy, Kumar, and Verma (2014), and for the two-dimensional case, Shebalin, Matthaeus, and Montgomery (1983)). It helps in the interpretation of Solar Wind data (Verdini, Grappin, Hellinger, Landi, & Müller, 2015), and has also applications in metallurgy: indeed, it is known that for sufficiently strong  $B_0$ , the fluid behaves like a quasi 2D three-component neutral fluid, the Lorentz force acting as an anisotropic dissipation (Garnier, Alemany, Sulem, & Pouquet, 1981), together with nonlocal energy transfers between the toroidal and poloidal components of the fields (Favier et al., 2011; Reddy et al., 2014). It is further found that the perpendicular components of the velocity undergo an upscale cascade whereas its parallel component follows a direct cascade, although this may depend on the strength of  $B_0$ . Such phenomena display a critical behavior (Sujovolsky & Mininni, 2016), the intensity of the magnetic fluctuations increasing as the one-half power of the Alfvén time based on the large-scale flow and on the uniform field. Furthermore, for strong  $B_0$ , the direct cascade is dominated by helicity (in relative terms), as in the rotating case (P. Mininni & Pouquet, 2009). It is not clear what happens when both rotation and an imposed uniform magnetic field are present, but the angle between these two imposed fields may alter the dynamics in significant ways. For example, it is shown in Salhi, Baklouti, Godeferd, Lehner, and Cambon (2017) that the Alfvén ratio (that is, the ratio of kinetic to magnetic energy in terms of radial spectra) has a different power-law decay for the parallel and orthogonal cases. It is seen moreover that quasi-equipartition recovers for wavenumbers such that the parameter  $V_A k$  be much larger than unity, with  $V_A = \sqrt{B_0^2/[\rho_0\mu_0]}$  the Alfvén velocity associated with the imposed magnetic field  $B_0$ , where  $\rho_0$  is the density taken as uniform, and  $\mu_0$  is the permeability of the vacuum. On the other hand, at large scale, the equipartition is between the kinetic and potential energy for  $V_A k/N$  much smaller than unity.

#### 4 The bi-directional, or dual, cascades in turbulence

Dual cascades have been observed in a variety of contexts, as in the ocean (Balwalda, LaCasce, & Speer, 2016; Klein et al., 2019; Sasaki, Klein, Qiu, & Sasai, 2014; Scott & Wang, 2005), in observations of the Solar Wind (Sorriso-Valvo et al., 2007) and of Jupiter (Young & Read, 2017), in experiments in a rotating tank (Morize, Moisy, & Rabaud, 2005) as well as in DNS of MHD flows (Alexakis, 2011) or of rotating flows (Kafabad & Bartello, 2016). The combination of direct and inverse energy cascades is invoked in the evolution and regeneration of wall turbulence (Farano, Cherubini, Robinet, & Palma, 2017), with the lifting of coherent structures in large-scale hairpin vortices which further destabilize and renew the (optimal) bursting cycles of such flows.

Rotating stratified turbulence (RST) is strongly anisotropic (see *e.g.*, Cambon and Jacquin (1989); Cambon and Scott (1999); Favier, Godeferd, Cambon, and Delache (2010)). In such flows, similarly to the MHD case, there is also a bi-directional constant-flux system of energy cascades to both the small scales and the large scales (Marino, Pouquet, & Rosenberg, 2015; Pouquet & Marino, 2013; Pouquet, Marino, Mininni, & Rosenberg, 2017). One can summarize these results, by analogy to MHD, in the following manner. In the atmosphere and the oceans, energy is injected through solar radiation, tides, bottom topography or winds for example. The large scales of such flows are in hydrostatic balance and in geostrophic balance between pressure gradient, Coriolis force and gravity. This leads to a quasi-2D behavior with the energy flowing to the large scales and thus without a clear way to dissipate the energy, a process which mostly takes place at small scale. What is, then, the internal mechanism for energy dissipation in such flows, outside of boundary layers, or considering the classical Ekman drag? In the presence of rotation, gravity as well as shear, several instabilities are known to exist; they take their energy from either the kinetic or the potential

modes (see Feraco et al. (2018); P. Wang, McWilliams, and Ménesguen (2014)). These instabilities can be viewed as the prelude to a direct cascade of energy to the small scales, with a constant flux, together with the inverse cascade. For atmospheric and oceanic dynamics, this split process for the energy cascade is essential.

In Figure 2 (top), we plot vorticity structures in rotating stratified turbulence with large-scale eddies due to the influence of rotation, at the border of which strong small-scale vortex lanes develop because of instabilities such as Kelvin-Helmoltz or those due to shear. The plot is for a flow with  $Re \approx 5.5 \times 10^4$ ,  $Fr \approx 0.024$ ,  $Ro \approx 0.1$ ,  $\mathcal{R}_B \approx 31$ , for a decay run on a grid of  $4096^3$  points, integrating the Boussinesq equations (see Rosenberg et al. (2015) and references therein for more details).

For a run with forcing centered on  $k_F \approx 10$  and a resolution of  $2048^3$  grid points (see Marino et al. (2015)), the relative helicity  $\sigma_V(k)$  is displayed in Fig. 2 (bottom left) at two different times, with the data displaced upward by a factor of 100 for clarity for the earlier time. Note that for this run, the buoyancy Reynolds number,  $\mathcal{R}_B = ReFr^2 \approx 313$  is quite high and the small-scale turbulence beyond the Ozmidov scale is close to the isotropic case. We see that  $\sigma_V(k)$  is quasi independent of wavenumber at large scales, in the inverse cascade, whereas it decays as  $\approx 1/k$  at scales smaller than the forcing, as it would for fully developed turbulence.

The bi-directional constant total energy flux, normalized by the kinetic energy dissipation  $\epsilon_V = \nu \langle |\boldsymbol{\omega}^2| \rangle$ , is displayed for several runs with parameters given in the inset in Fig. 2 (middle plot). Buoyancy Reynolds numbers vary between roughly 31 and 313 (black curve), with Reynolds numbers high enough that the small-scale fluxes are rather well-developed and approximately constant. As analyzed in Marino et al. (2015); Pouquet and Marino (2013); Pouquet et al. (2017), the ratio of the forward to inverse flux varies as  $[RoFr]^{-1}$  as long as the Rossby number is below unity and for buoyancy Reynolds numbers  $\mathcal{R}_B$  above a threshold of order 10. Note that the analysis of the forced case was also shown to be compatible with the energy flux to the small scales being proportional to  $Fr$ , when the (total) energy flux to the large scale was inversely proportional to the Rossby number  $Ro$ : at fixed Froude number, the stronger the rotation, the more the energy flows to the large scales.

Finally, at the bottom right of Fig. 2 is given again the total energy flux, but this time with a forcing in quasi-geostrophic balance. This run is forced with a classical Taylor-Green (TG) flow with  $\mathbf{F}^u_{TG} = [\sin x \cos y \cos z, -\cos x \sin y \cos z, 0]$ .  $\mathbf{F}^u_{TG}$  is incompressible, has zero vertical component and zero total helicity. The forcing in the temperature equation is such that it is in geostrophic balance with the TG flow (see Rosenberg et al. (2015)). The dimensionless parameters for this run are  $Re \approx 2500$ ,  $Fr \approx 0.09$ ,  $\mathcal{R}_B \approx 20$ ,  $N/f \approx 2.02$ ,  $Ro \approx 0.18$ , with  $N = 18.6$ , and the grid resolution is  $512^3$ . The run is comparable to the forced run 10e studied in Marino et al. (2015); Pouquet and Marino (2013), but at a lower Reynolds number; thus, the direct flux is competing with dissipation and is not constant at that resolution, but it confirms the generality of the bi-directional cascades in RST for different initial conditions.

It is becoming increasingly clear that the role of large-scale shear is central in many turbulent flows (Pumir, 1996), as in the structure of late-time coherent eddies in 2D (Frishman, 2017; Frishman & Herbert, 2018), in the destabilization of stratified flows as discussed above (see Fig. 2, top), or when it leads to the formation of fronts between meta-stable and stable states, or between quiet and turbulent regions (Pomeau, 1986; Waleffe, 1997). The connection, in the context of the dynamics between large-scale predator (the shear flow) and prey (the turbulent eddies), and in which the details of the small-scale turbulent eddies are rather irrelevant, allows for the classification of turbulent flows by analogy with directed percolation (Barkley, 2016; Pomeau, 2015), as supported by laboratory experiments (Sano & Tamai, 2016). Indeed, the critical transition to a turbulent state has exponents comparable to those



of directed percolation, concerning for example the scaling of the number of active sites in terms of distance to the critical governing parameter of the transition. Such an analysis also shows the importance of large-scale zonal flows (Shih, Hsieh, & Goldensfeld, 2016), of critical layers (Park, Shekar, & Graham, 2018), as well as that of regeneration self-sustaining cycles in such flows (Kawahara & Kida, 2001; Waleffe, 1997) with, citing McKeon (2017), “*the importance of scale interactions in sustaining wall turbulence through the non-linear term.*”

In terms of oceanic dynamics, the instabilities giving rise to the forward transfer of energy are often identified as sub-meso-scale currents at scales of  $1\text{ km}$  which have been recently discovered in the ocean (see McWilliams (2016) for a recent review), and which, in general, are hard to obtain numerically for lack of resolution in global simulations. They may occur in the boundary layers and, if unstable (which they likely are) will provide a path to small dissipative scales, taking the form of eddies, fronts or jets, and filaments. The oceanic observations analyzed in Arbic, Polzin, Scott, Richman, and Shriver (2013) indicate as well the existence of a split bi-directional flux. Such a dual-cascade system can also be viewed as two independent cascades corresponding to the geostrophic and ageostrophic parts of the flow (Bartello, 1995).

In fully developed turbulent flows, it is shown in Djenidi, Lefeuvre, Kamruzzaman, and Antonia (2017); Ishihara et al. (2016) that the effective amount of kinetic energy dissipation, measured in terms of its dimensional evaluation  $\epsilon_D = U_0^3/L_0$ , tends to a constant close to  $1/2$  for a variety of laboratory and numerical experiments, in the forced case as well as for decaying flows provided their Taylor Reynolds numbers be sufficiently high, but there is also a marked deficiency, of the order of 10%, in the presence of non-zero helicity (Linkmann, 2018). The actual amount of dissipation (as opposed to that expected for a field composed of a superposition of linear waves interacting weakly), directly influences the overall atmospheric and oceanic energetic exchanges, and it can also modify conditions for acoustic transmission, as well as for deep-water drilling. Dissipation and wave effects are thus important features of such flows to be determined. The presence of waves affects directly turbulent flows in lessening the rate at which energy is dissipated. It has been observed in several instances (Alexakis, 2013; Campagne, Machicoane, Gallet, Cortet, & Moisy, 2016; Feraco et al., 2018; Maffioli, Brethouwer, & Lindborg, 2016; Pouquet et al., 2017), with in the case of rotating stratified flows, a clear linear dependence of the measured dissipation on the control parameter, the Froude number in an intermediate regime of eddy-wave interactions (Marino et al., 2015; Pouquet, Rosenberg, Marino, & Herbert, 2018). On the other hand, the Rossby number controls the amount of energy going to the large scales in a simultaneous inverse cascade, whereas for MHD the control parameter is the magnitude of the large-scale imposed magnetic field. It is also shown, both for MHD (Alexakis, 2013) and for RST (Pouquet et al., 2018; Rosenberg, Marino, Herbert, & Pouquet, 2016) that the two forms of dissipation (kinetic and magnetic, or kinetic and potential) can become comparable. In convectively-forced rotating turbulence, using experiments with helium performed in a cylinder of aspect ratio  $1/2$ , Ecke and Niemela (2014) find a similar linear scaling for the flux measured through the Nusselt number (normalized by its non-rotating value for the same parameters). Finally, we note that the transition between regimes where either vortices or waves are the dominant modes can be analyzed, in the case of purely rotating flows, in terms of the elliptical instability (Le Reun, Favier, Barker, & Le Bars, 2017). This can justify the presence of turbulence in planetary interiors, which can in turn lead to a dynamo mechanism for the generation of planetary magnetic fields.

## 5 Conclusion and Perspectives

The study of turbulence, for fluids and MHD, and of nonlinear systems in general, is progressing substantially as shown, among others, in the few examples given in the

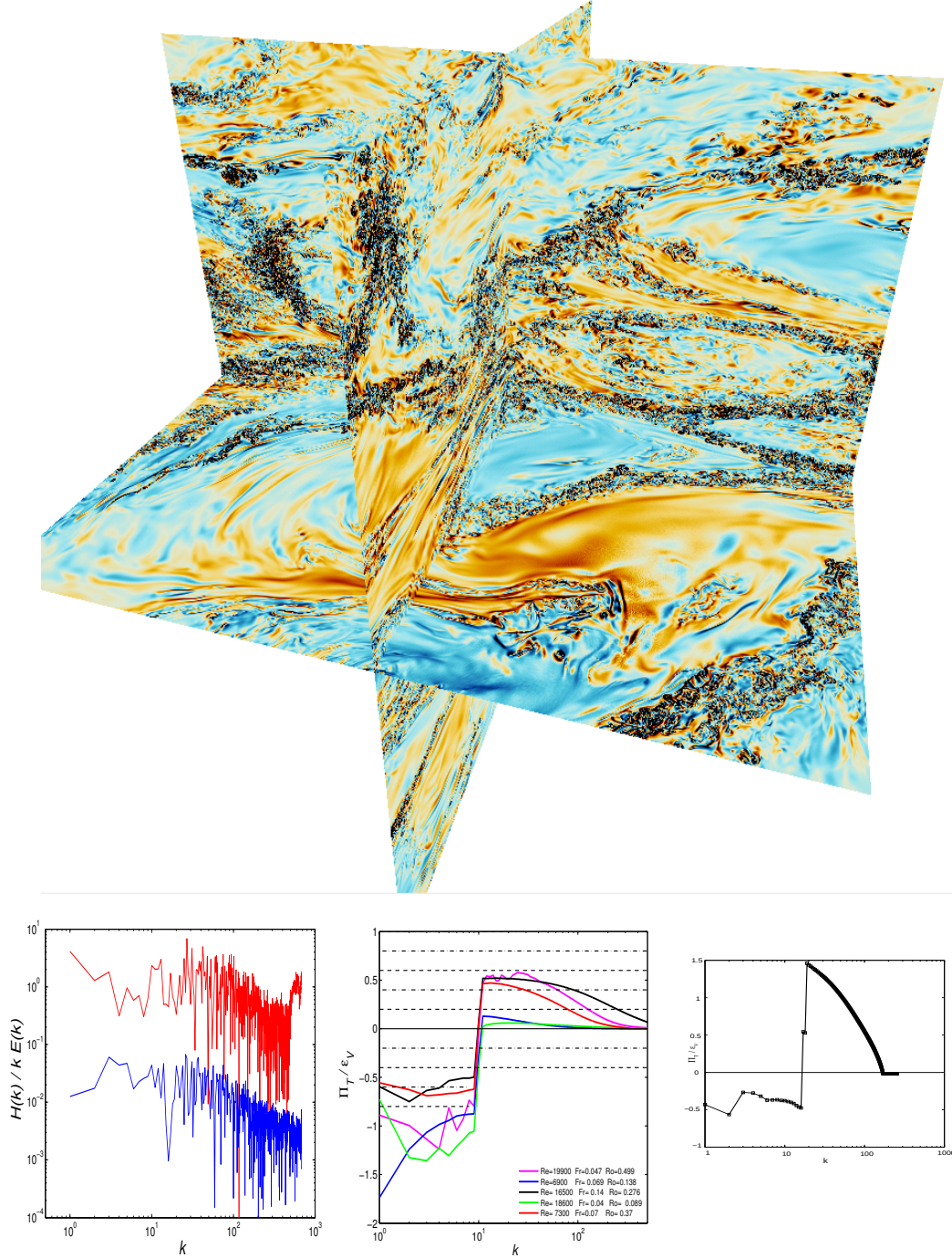


**Figure 2.** *Rotating stratified flows.* *Top:* Vorticity strength on three planes for the decay run analyzed in Rosenberg et al. (2015), where the color map is also given. The grid has  $4096^3$  points,  $N/f = 5$ ,  $Re = 55,000$ ,  $Fr = 0.024$ . *Bottom left:* Relative helicity spectra at two different times for runs analyzed in Marino et al. (2015) on grids of  $2048^3$  points,  $Re \approx 1.65 \times 10^4$ ,  $N/f = 2$ ,  $Fr \approx 0.14$ . For clarity, the data has been shifted upward by a factor 100 for the earlier time (in red). *Bottom middle:* Energy fluxes with dual cascades for isotropic forcing in the velocity only, grids of  $1024^3$  or  $2048^3$  points for runs analyzed in Marino et al. (2015); Pouquet and Marino (2013); the parameters are given in the inset. *Bottom right:* Dual cascade energy flux for quasi-geostrophic forcing for a new run; grid of  $512^3$  points,  $Re \approx 2500$ ,  $Fr \approx 0.09$ ,  $N/f = 1.97$ . All fluxes are averaged for several turn-over times after the onset of the inverse cascade.

preceding sections. Turbulence studies also lead to the existence of large data sets. An existing approach to reduce the complexity of the problem has been to identify regions of strong turbulent activity in coherent structures, such as with a principal orthogonal decomposition (see Mezić (2013) for a recent review), through intermittency or by examining enhanced dissipation such as in current sheets, and concentrate the analysis on such regions. When contemplating the vorticity field (Ishihara et al., 2016), computed on a grid of  $4096^3$  points (or in excess of 64 billion points), it becomes apparent that the information content of such a picture is enormous, and the dynamics of the fields on this large grid is computed with spectral accuracy. Analysis of such large data sets is cumbersome. Local mesh refinement can help in the analysis of sporadic, intermittent structures which are at the basis of the strong and recurrent increases in kurtosis in stratified flows (Feraco et al., 2018). For example, a comparison of spectral element and finite difference methods using statically refined nonconforming grids for the MHD island coalescence instability problem led to the conclusion that a high degree of accuracy is, perhaps unsurprisingly, helpful in identifying correctly the spatio-temporal localization of strong current structures (Ng, Rosenberg, Germaschewski, Pouquet, & Bhattacharjee, 2008).

Can we do better than increasing the grid size? In other words, is there another way out? Little has been done in the field of turbulence using techniques such as data neural networks, although we already have some pieces of information. Machine Learning (ML) has now been used in fluid turbulence (Duriez, Brunton, & Noack, 2017), with possible applications to drag reduction for cars, trucks and ships through active turbulent flow control mechanisms. Other applications include the re-“discovery” of the underlying equations from experimental and/or numerical data (Brunton, Brunton, Proctor, Kaiser, & Kutz, 2017), the development of new and improved sub-grid scale modeling (Kutz, 2017; Ling, Kurzawski, & Templeton, 2016), the prediction of long-time behavior of chaotic systems (Pathak, Hunt, Girvan, Lu, & Ott, 2018), and specifically that of earthquakes (DeVries, Viégas, Wattenberg, & Meade, 2018; Rouet-Leduc et al., 2017).

Various physics-based model enhancements have already been proposed, as for example incorporating helicity-dependent eddy diffusivities (Baerenzung et al., 2008) including in the case of shear flows (Yokoi & Brandenburg, 2016), or when helicity leads to large-scale instabilities (Frisch et al., 1987), or for models including the potential energy for RST (Zilitinkevich et al., 2008). One application will be to illuminate the possible connections to climate between atmospheric and oceanic dynamics, as well as human interferences (Rockström et al., 2009; Steffen et al., 2015).

Similarly, the controlling of uncertainties in Reynolds-Averaged Navier-Stokes high-fidelity models can be accomplished through the use of large numerical simulations, either directly exploiting large turbulence data bases (Duraismy, Iaccarino, & Xiao, 2018; Graham et al., 2016; J.-X. Wang, Wu, & Xiao, 2017), or with Large-Eddy Simulations. It may also inform the functional form of the closure schemes, as well as the actual values of the coefficients appearing in such closures. Extreme weather events can also be predicted using instantaneous dynamical system metrics, linked in particular to the rapidity of nearby trajectories in phase-space to diverge (Messori, Caballero, & Faranda, 2017).

These approaches are rather unexplored in MHD. Automatized current structure identification was performed in Klimas and Uritsky (2017); Servidio et al. (2010) for 2D MHD flows by detecting nulls of the magnetic field with a local hyperbolic topology as the plausible locus of reconnection events. Similarly, one can observe geo-dynamo field reversals using a decomposition of the data through a chaotic forcing with strong intermittent bursts (Brunton et al., 2017). Finally, Lagrangian models (also called  $\alpha$ -models) allow for computations at high Reynolds numbers by introducing a filter length-scale. These models can, for example, lead to accurate evaluations of sign-

cancellations in 2D MHD, leading to the prediction of that exponent being independent of Reynolds number at high Reynolds numbers (Graham, Mininni, & Pouquet, 2005). However, this sharp truncation using the  $\alpha$  parameter may lead to extended regions of very weak nonlinear transfer (P. D. Mininni, Montgomery, & Pouquet, 2005), and Machine Learning procedures could alleviate that problem. One could also think of incorporating cross-helicity and/or magnetic helicity in transport coefficients for MHD, following similar venues.

Artificial intelligence has been used recently in helping develop more efficient fusion devices that avoid disrupting the magnetically-confined plasmas (see Camporeale, Wing, Johnson, Jackman, and McGranaghan (2018) for space weather). Data-driven predictions of large-scale disruptions, now at a level of 90% accuracy, does allow for early plasma-device shut-down through pattern recognition applied to previous events (there is close to half a peta-byte of data). These disruptions are associated with wall-driven MHD resistive instabilities (Vega et al., 2014), and such a classification of events can be physics-based and multi-dimensional (Tang, Parsons, Feibush, Choi, & Kurc, 2017). The disruptions are also related to the burstiness of the turbulence leading to localized anomalous transport in plasmas (Diamond, Liang, Carreras, & Terry, 1994), which can be modeled through avalanche dynamics (Hahm & Diamond, 2018).

In what way will existing machine learning algorithms change in the presence of inverse cascades? How will such modeling be affected by the existence of bi-directional cascades? Much remains to be learned but it seems rather certain that Big Data and Data Science will play a role in MHD turbulence in perhaps much the same way as it has demonstrated its utility in other fields. These issues could be investigated soon with the existence, as mentioned earlier, of new observational small-scale data with the Multiscale Magnetospheric mission (Chasapis et al., 2017; Ergun et al., 2018; Gershman et al., 2018; Wilder et al., 2016)), with experimental data (*e.g.*, coming from the Coriolis table (Aubourg et al., 2017)), and with numerical data stemming from high-performance computing studies of FDT (Ishihara et al., 2016), of rotating and/or stratified turbulence (de Bruyn Kops, 2015; Rosenberg et al., 2015), as well as of turbulent interfaces in RST (Watanabe, Riley, de Bruyn-Kops, Diamessis, & Zhou, 2016), and of MHD turbulence (Beresniak, 2014; Lee et al., 2010; Zhai & Yeung, 2018).

### Acknowledgments

Support for AP from LASP, and in particular from Bob Ergun, is gratefully acknowledged. JES is supported by STFC(UK) grant ST/N000692/1. RM acknowledges financial support from PALSE (Programme Avenir Lyon Saint-Etienne) of the University of Lyon, in the framework of the program “Investissements d’Avenir” (ANR-11-IDEX-0007). Computations were performed at LASP, on the Janus supercomputer at the University of Colorado (Boulder) for Fig. 1, at DOE for Fig. 2 (top), and on local servers for Fig. 2 (bottom). We thank all such centers. NCAR is supported by NSF. We want to remark that a comprehensive review on closely related topics has just appeared (Alexakis & Biferale, 2018). Finally, data for Fig. 2 (top) is available on the Turbulence data base at John Hopkins University (Graham et al., 2016); the much smaller data sets used for the other plots are available directly from the authors.

### References

- Abramenko, V., & Yurchyshyn, V. (2010). Intermittency and multifractality spectra of the magnetic field in solar active regions. *Astrophys. J.*, *722*, 122-130.
- Alexakis, A. (2011). Two-dimensional behavior of three-dimensional magnetohydrodynamic flow with a strong guiding field. *Phys. Rev. E*, *84*, 056330.
- Alexakis, A. (2013). Large-scale magnetic fields in magnetohydrodynamic turbu-



- lence. *Phys. Rev. Lett.*, *110*, 084502.
- Alexakis, A. (2017). Helically decomposed turbulence. *J. Fluid Mech.*, *812*, 752-770.
- Alexakis, A. (2018). 3D instabilities and negative eddy viscosity in thin-layer flows. *Preprint*, see *ArXiv:1806.00409v1*.
- Alexakis, A., & Biferale, L. (2018). Cascades and transitions in turbulent flows. *Physics Reports*, *762*, 1-139.
- Alexakis, A., Mininni, P., & Pouquet, A. (2006). On the inverse cascade of magnetic helicity. *Astrophys. J.*, *640*, 335-343.
- Alexandrova, O., Mangeney, A., Maksimovic, M., Cornilleau-Wehrlin, N., Bosqued, J.-M., & André, M. (2006). Alfvén vortex filaments observed in magnetosheath downstream of a quasi-perpendicular bow shock. *J. Geophys. Res.*, *111*(A12208).
- Arbic, B., Polzin, K., Scott, R., Richman, J., & Shriver, J. (2013). On eddy viscosity, energy cascades, and the horizontal resolution of gridded satellite altimeter products. *J. Phys. Oceano.*, *43*, 283-300.
- Aubourg, Q., Campagne, A., Peureux, C., Arduin, F., Sommeria, J., Viboud, S., & Mordant, N. (2017). Three-wave and four-wave interactions in gravity wave turbulence. *Phys. Rev. Fluids*, *2*, 114802.
- Azpiroz-Zabala, M., Cartigny, M. J. B., Sumner, E. J., Clare, M. A., Talling, P. J., Parsons, D. R., & Cooper, C. (2017). A general model for the helical structure of geophysical flows in channel bends. *Geophys. Res. Lett.*, *44*, 11,932-11,941.
- Baerenzung, J., Mininni, P., Pouquet, A., & Rosenberg, D. (2011). Spectral modeling of turbulent flows and the role of helicity in the presence of rotation. *J. Atmos. Sci.*, *68*, 2757-2770.
- Baerenzung, J., Politano, H., Ponty, Y., & Pouquet, A. (2008). Spectral modeling of turbulent flows and the role of helicity. *Phys. Rev. E*, *77*, 046303.
- Baker, N. T., Pothérat, A., Davoust, L., & Debray, F. (2018). Inverse and direct energy cascades in three-dimensional magnetohydrodynamic turbulence at low magnetic Reynolds number. *xx*, *120*, 224502.
- Balwada, D., LaCasce, J., & Speer, K. (2016). Scale-dependent distribution of kinetic energy from surface drifters in the Gulf of Mexico. *Geophys. Res. Lett.*, *43*, 10,856-10,863.
- Barkley, D. (2016). Theoretical perspective on the route to turbulence in a pipe. *J. Fluid Mech.*, *803*, *PI*, 1-80.
- Bartello, P. (1995). Geostrophic adjustment and inverse cascade in rotating stratified turbulence. *J. Atmos. Sci.*, *52*, 4410-4428.
- Beresniak, A. (2014). Spectra of strong magnetohydrodynamic turbulence from high resolution simulations. *Astrophys. J. Lett.*, *784*(L20).
- Biferale, L., Musacchio, S., & Toschi, F. (2012). Inverse energy cascade in three-dimensional isotropic turbulence. *Phys. Rev. Lett.*, *108*, 164501.
- Biferale, L., & Titi, E. (2013). On the global regularity of a helical-decimated version of the 3D Navier-Stokes equations. *J. Stat. Phys.*, *151*, 1089-1098.
- Blackman, E. (2015). Magnetic helicity and large scale magnetic fields: A primer. *Space Sci. Rev.*, *8*.
- Bose, R., & Durbin, P. A. (2016). Helical modes in boundary layer transition. *Phys. Rev. Fluids*, *1*(073602).
- Brandenburg, A., & Subramanian, K. (2005). Astrophysical magnetic fields and nonlinear dynamo theory. *Phys. Rep.*, **417**(1).
- Bratanov, V., Jenko, F., Hatch, D. R., & Wilczek, M. (2013). Non-universal power-law spectra in turbulent systems. *Phys. Rev. Lett.*, *111*, 075001.
- Briard, A., & Gomez, T. (2018). The decay of isotropic magnetohydrodynamic turbulence and the effects of cross-helicity. *J. Plasma Phys.*, *84*, 905840110.
- Brunton, S. L., Brunton, B. W., Proctor, J. L., Kaiser, E., & Kutz, J. N. (2017). Chaos as an intermittently forced linear system. *Nature Comm.*, *8*, 1-9.
- Burch, J. L., Torbert, R. B., Phan, T. D., Chen, L.-J., Moore, T. E., Ergun, R. E.,

- ... Chandler, M. (2016). Electron-scale measurements of magnetic reconnection in space. *Science*, *352*(6290). doi: 10.1126/science.aaf2939
- Cambon, C., & Jacquin, L. (1989). Spectral approach to non-isotropic turbulence subjected to rotation. *J. Fluid Mech.*, *202*, 295-317.
- Cambon, C., & Scott, F. (1999). Linear and nonlinear models of anisotropic turbulence. *Ann. Rev. Fluid Mech.*, *31*, 1-53.
- Campagne, A., Machicoane, N., Gallet, B., Cortet, P. P., & Moisy, F. (2016). Turbulent drag in a rotating frame. *J. Fluid Mech.*, *794*, R5.
- Camporeale, E., Wing, S., Johnson, J., Jackman, C., & McGranaghan, R. (2018). Space weather in the machine learning era: A multidisciplinary approach. *Space Weather*, *16*, 2-4.
- Canet, L., Delamotte, B., & Wschebor, N. (2016). Fully developed isotropic turbulence: Non-perturbative renormalization group formalism and fixed-point solution. *Phys. Rev. E*, *93*(063101).
- Cassak, P. A., Emslie, A. G., Halford, A. J., Baker, D. N., Spence, H. E., Avery, S. K., & Fisk, L. A. (2017). Space physics and policy for contemporary society. *J. Geophys. Res.*, *122*, 1-6.
- Castellano, C., Fortunato, S., & Loreto, V. (2009). Statistical physics of social dynamics. *Rev. Mod. Phys.*, *81*, 591-646.
- Chasapis, C., Matthaeus, W. H., Parashar, T. N., Fuselier, S. A., Maruca, B. A., Phan, T. D., ... Strangeway, R. J. (2017). High-resolution statistics of Solar Wind turbulence at kinetic scales using the Magnetospheric Multiscale Mission. *Astrophys. J. Lett.*, *844*, L9.
- Chatterjee, G., Schoeffler, K. M., Singh, P. K., Adak, A., Lad, A. D., Sengupta, S., ... Kuma, G. R. (2017). Magnetic turbulence in a table-top laser-plasma relevant to astrophysical scenarios. *Nature Phys.*, *13*, 8:15970.
- Che, H., Goldstein, M., & Viñas, A. (2014). Bidirectional energy cascades and the origin of kinetic Alfvénic and whistler turbulence in the solar wind. *Phys. Rev. Lett.*, *112*, 061101.
- Chen, Q., Chen, S., & Eyink, G. (2003). The joint cascade of energy and helicity in three-dimensional turbulence. *Phys. Fluids*, *15*, 361-374.
- Childress, S., & Gilbert, A. D. (1995). *Stretch, twist, fold: The fast dynamo* (Vol. 37). Springer.
- Cho, J. (2011). Magnetic helicity conservation and inverse energy cascade in electron magnetohydrodynamic wave packets. *Phys Rev. Lett.*, *106*, 191104.
- Choi, Y., Lvov, Y., Nazarenko, S., & Pokorni, B. (2005). Anomalous probability of large amplitudes in wave turbulence. *Phys. Lett. A*, *339*, 361-369.
- Clark di Leoni, P., Cobelli, P., & Mininni, P. D. (2015). The spatio-temporal spectrum of turbulent flows. *Eur. Phys. J. E*, *38*, 136.
- Clark di Leoni, P., Mininni, P. D., & Brachet, M. E. (2017). Dual cascade and dissipation mechanisms in helical quantum turbulence. *Phys. Rev. A*, *95*, 053636.
- Constantinescu, G., Miyawaki, S., Rhoads, B., Sukhodolov, A., & Kirkil, G. (2011). Structure of turbulent flow at a river confluence with momentum and velocity ratios close to 1: Insight provided by an eddy-resolving numerical simulation. *Water Resources Res.*, *47*(W05507), 1-16.
- Dallas, V., & Alexakis, A. (2015). Self-organisation and non-linear dynamics in driven magnetohydrodynamic turbulent flows. *Phys. Fluids*, *27*, 045105.
- Davidson, P. (2013). *Turbulence in rotating, stratified and electrically conducting fluids*. Cambridge University Press.
- Debliqy, O., Verma, M., & Carati, D. (2005). Energy fluxes and shell-to-shell transfers in three-dimensional decaying magnetohydrodynamic turbulence. *Phys. Plasmas*, *12*(042309).
- de Bruyn Kops, S. (2015). Classical scaling and intermittency in strongly stratified Boussinesq turbulence. *J. Fluid Mech.*, *775*, 436-463.
- DeVries, P. M. R., Viégas, F., Wattenberg, M., & Meade, B. J. (2018). Deep learn-



- ing of aftershock patterns following large earthquakes. *Nature*, *560*, 632-647.
- Dewan, E. (1997). Saturated-cascade similitude theory of gravity wave spectra. *J. Geophys. Res.*, *102*, 29,799-29,817.
- Diamond, P. H., Liang, Y.-M., Carreras, B. A., & Terry, P. (1994). Self-regulating shear flow turbulence: A paradigm for the L to H transition. *Phys. Rev. Lett.*, *72*, 2565-2568.
- Djenidi, L., Lefeuvre, N., Kamruzzaman, M., & Antonia, R. (2017). On the normalized dissipation  $c_\epsilon$  in decaying turbulence. *J. Fluid Mech.*, *817*, 61-79.
- Dombrowski, C., Cisneros, L., Chatkaew, S., Goldstein, R. E., & Kessler, J. O. (2004). Self-concentration and large-scale coherence in bacterial dynamics. *Phys. Rev. Lett.*, *93*, 098103.
- Duraisamy, K., Iaccarino, G., & Xiao, H. (2018). Turbulence modeling in the age of data. *Ann. Rev., preprint, ArXiv:1804:00183v1*, 1-23.
- Duriez, T., Brunton, S. L., & Noack, B. R. (2017). *Machine learning control – taming nonlinear dynamics and turbulence* (Vol. 116). Springer.
- Ecke, R. E., & Niemela, J. J. (2014). Heat transport in the geostrophic regime of rotating Rayleigh-Bénard convection. *Phys. Rev. Lett.*, *113*(114301).
- Ergun, R. E., Goodrich, K. A., Wilder, F. D., Ahmadi, N., Holmes, J. C., Eriksson, S., . . . Vaivads, A. (2018). Magnetic reconnection, turbulence, and particle acceleration: Observations in the Earth’s magnetotail. *Geophys. Res. Lett.*, *45*, 3338-3347.
- Farano, M., Cherubini, S., Robinet, J.-C., & Palma, P. D. (2017). Optimal bursts in turbulent channel flow. *J. Fluid Mech.*, *817*, 35-60.
- Favier, B., Godeferd, F., Cambon, C., Delache, A., & Bos, W. (2011). Quasi-static magnetohydrodynamic turbulence at high Reynolds number. *J. Fluid Mech.*, *681*, 434-461.
- Favier, B., Godeferd, F. S., Cambon, C., & Delache, A. (2010). On the two-dimensionalization of quasistatic magnetohydrodynamic turbulence. *Phys. Fluids*, *22*, 075104.
- Feraco, F., Marino, R., Pumir, A., Primavera, L., Mininni, P., Pouquet, A., & Rosenberg, D. (2018). Vertical drafts and mixing in stratified turbulence: sharp transition with Froude number. *Eur. Phys. Lett.*, *123*, 44002.
- Fjørtoft, R. (1953). On the changes in the spectral distribution of kinetic energy for two-dimensional non-divergent flows. *Tellus*, *5*, 225-230.
- Frisch, U., Pouquet, A., Léorat, J., & Mazure, A. (1975). Possibility of an inverse cascade of magnetic helicity in magnetohydrodynamic turbulence. *J. Fluid Mech.*, *68*, 769-778.
- Frisch, U., She, Z., & Sulem, P. (1987). Large-scale flow driven by the anisotropic kinetic alpha effect. *Physica D*, *28*, 382-392.
- Frishman, A. (2017). The culmination of an inverse cascade: Mean flow and fluctuations. *Phys. Fluids*, *29*(125102).
- Frishman, A., & Herbert, C. (2018). Turbulence statistics in a two-dimensional vortex condensate. *Phys. Rev. Lett.*, *120*(204505).
- Fyfe, D., & Montgomery, D. (1976). High beta turbulence in two-dimensional magnetohydrodynamic. *J. Plasma Phys.*, *16*, 181-191.
- Gallet, B., & Doering, C. R. (2015). Exact two-dimensionalization of low-magnetic-Reynolds-number flows subject to a strong magnetic field. *J. Fluid Mech.*, *773*, 154-177.
- Galtier, S. (2012). Kolmogorov vectorial law for Solar Wind turbulence. *Astrophys. J.*, *746*, 184.
- Galtier, S. (2016). *Introduction to modern magnetohydrodynamics*. Cambridge University Press.
- Galtier, S., & Bhattacharjee, A. (2003). Anisotropic weak whistler wave turbulence in electron magnetohydrodynamics. *Phys. Plasmas*, *10*, 3065-3076.
- Galtier, S., & Meyrand, A. (2015). Entanglement of helicity and energy in kinetic

- alfvén wave/whistler turbulence. *J. Plasma Phys.*, *81*, 325810106.
- Garnier, M., Alemany, A., Sulem, P. L., & Pouquet, A. (1981). Influence of an external magnetic field on large scale Reynolds number MHD turbulence. *J. de Mécanique*, *20*, 233-251.
- Gershman, D. J., F.-Viñas, A., Dorelli, J. C., Goldstein, M. L., Shuster, J., Avakov, L. A., . . . Burch, J. L. (2018). Energy partitioning constraints at kinetic scales in low- $\beta$  turbulence. *Phys. Plasmas*, *25*, 022303.
- Gibson, S., & Fan, Y. (2008). Partially ejected flux ropes: Implications for interplanetary coronal mass ejections. *J. Geophys. Res.*, *113*, A09103.
- Gomez, T., Politano, H., & Pouquet, A. (2000). An exact relationship for third-order structure functions in helical flows. *Phys. Rev. E*, *61*, 5321-5325.
- Graham, J., Kanov, K., X.I.A. Yang, Lee, M., Malaya, N., Lalescu, C., . . . Meneveau, C. (2016). A Web services accessible database of turbulent channel flow and its use for testing a new integral wall model for LES. *J. Turbulence*, *17*, 181-215.
- Graham, J., Mininni, P. D., & Pouquet, A. (2005). Cancellation exponent and multifractal structure in Lagrangian averaged magnetohydrodynamics. *Phys. Rev. E*, *72*, 045301(R).
- Gustavsson, K., & Biferale, L. (2016). Preferential sampling of helicity by isotropic helicoids. *Phys. Rev. F*, *1*, 054201.
- Hahm, T., & Diamond, P. (2018). Mesoscopic transport events and the breakdown of Fick's law for turbulent fluxes. *J. Korean Phys. Soc.*, *73*, 747-792.
- Henri, P., Califano, F., Briand, C., & Mangeney, A. (2011). Low-energy Langmuir cavitons: Asymptotic limit of weak turbulence. *Eur. J. Phys. Lett.*, *96*, 55004.
- Hide, R. (2002). Helicity, superhelicity and weighted relative potential vorticity: Useful diagnostic pseudoscalars? *Q. J. Roy. Met. Soc.*, *128*, 1759-1762.
- Higashimori, K., Yokoi, N., & Hoshino, M. (2013). Explosive turbulent magnetic reconnection. *Phys. Rev. Lett.*, *110*(255001).
- Howes, G., & Quataert, E. (2010). On the interpretation of magnetic helicity signatures in the dissipation range of Solar Wind turbulence. *Astrophys. J. Lett.*, *709*, L49-L52.
- Ishihara, T., Morishita, K., Yokokawa, M., Uno, A., & Kaneda, Y. (2016). Energy spectrum in high-resolution direct numerical simulations of turbulence. *Phys. Rev. F*, *1*(082403(R)).
- Iyer, K. P., Sreenivasan, K. R., & Yeung, P. K. (2017). Reynolds number scaling of velocity increments in isotropic turbulence. *Phys. Rev. E*, *95*, 021101(R).
- Kafiabad, H., & Bartello, P. (2016). Balance dynamics in rotating stratified turbulence. *J. Fluid Mech.*, *795*, 914-949.
- Karimabadi, H., Roytershteyn, V., Wan, M., Matthaeus, W. H., Daughton, W., Wu, P., . . . Nakamura, T. K. M. (2013). Coherent structures, intermittent turbulence, and dissipation in high-temperature plasmas. *Phys. Plasmas*, *20*, 012303.
- Kawahara, G., & Kida, S. (2001). Periodic motion embedded in plane Couette turbulence: regeneration cycle and burst. *J. Fluid Mech.*, *449*, 291-300.
- Kerr, R. (1985). Higher order derivative correlations, the alignment of small-scales structures in isotropic numerical turbulence. *J. Fluid Mech.*, *153*, 31-58.
- Kerr, R. (1987). Histograms of helicity in numerical turbulence. *Phys. Rev. Lett.*, *59*, 783-786.
- Kim, H., & Cho, J. (2015). Inverse cascade in imbalanced electron magnetohydrodynamic turbulence. *Astrophys. J. Suppl.*, *801*, 75.
- Klein, P., Lapeyre, G., Siegelman, L., Torres, H., Su, Z., & Smith, S. K. (2019). Ocean scale interactions from space, to appear. *Earth Space Sci.*
- Klimas, A. J., & Uritsky, V. M. (2017). Criticality and turbulence in a resistive magnetohydrodynamic current sheet. *Phys. Rev. E*, *95*, 023209.
- Koprov, B., Koprov, V., Ponomarev, V., & Chkhetiani, O. (2005). Experimental

- studies of turbulent helicity and its spectrum in the atmospheric boundary layer. *Dokl. Phys.*, *50*, 419-422.
- Kraichnan, R. (1967). Inertial ranges in two-dimensional turbulence. *Phys. Fluids*, *10*, 1417-1423.
- Kraichnan, R. (1973). Helical turbulence and absolute equilibrium. *J. Fluid Mech.*, *59*, 745-752.
- Kraichnan, R. (1994). Anomalous scaling of a randomly advected passive scalar. *Phys. Rev. Lett.*, *72*, 1016-1019.
- Kutz, J. (2017). Deep learning in fluid dynamics. *J. Fluid Mech.*, *814*, 1-4.
- Le Reun, T., Favier, B., Barker, A. J., & Le Bars, M. (2017). Inertial wave turbulence driven by elliptical instability. *Phys. Rev. Lett.*, *119*, 034502.
- Lee, E., Brachet, M., Pouquet, A., Mininni, P., & Rosenberg, D. (2010). On the lack of universality in decaying magnetohydrodynamic turbulence. *Phys. Rev. E*, *81*, 016318.
- Lessines, T., Plunian, F., & Carati, D. (2009). Helical shell models for MHD. *Theor. Comput. Fluid Dyn.*, *23*, 439-450.
- Levina, G., & Montgomery, M. (2014). Tropical cyclogenesis: a numerical diagnosis based on helical flow organization. *J. Phys: Conf. Ser.*, *544*, 012013.
- Ling, J., Kurzawski, A., & Templeton, J. (2016). Reynolds averaged turbulence modelling using deep neural networks with embedded invariance. *J. Fluid Mech.*, *807*, 155-166.
- Linkmann, M. (2018). Effects of helicity on dissipation in homogeneous box turbulence. *J. Fluid Mech.*, *856*, 79-102.
- Linkmann, M., Buzzicotti, M., & Biferale, L. (2018). Non-universal behaviour of helical two-dimensional three-component turbulence. *Eur. J. Phys. E*, *41*, 4.
- Linkmann, M., & Dallas, V. (2017). Triad interactions and the bidirectional turbulent cascade of magnetic helicity. *Phys. Rev. F*, *2*, 054605.
- Linkmann, M., Sahoo, G., McKay, M., Berera, A., & Biferale, L. (2017). Effects of magnetic and kinetic helicities on the growth of magnetic fields in laminar and turbulent flows by Fourier helical decomposition. *Astrophys. J.*, *26*, 836.
- Loureiro, N. F., Schekochihin, A. A., & Uzdensky, D. A. (2013). Plasmoid and Kelvin-Helmholtz instabilities in Sweet-Parker current sheets. *Phys. Rev. E*, *87*, 013102.
- Maffioli, A., Brethouwer, G., & Lindborg, E. (2016). Mixing efficiency in stratified turbulence. *J. Fluid Mech.*, *794*, R3.
- Malapaka, S., & Müller, W. (2013). Modeling statistical properties of solar active regions through direct numerical simulations of 3D-MHD turbulence. *Astrophys. J.*, *774*, 84.
- Marino, R., Mininni, P., Rosenberg, D., & Pouquet, A. (2013). Emergence of helicity in rotating stratified turbulence. *Phys. Rev. E*, *87*, 033016.
- Marino, R., Pouquet, A., & Rosenberg, D. (2015). Resolving the paradox of oceanic large-scale balance and small-scale mixing. *Phys. Rev. Lett.*, *114*, 114504.
- Marino, R., Sorriso-Valvo, L., Carbone, V., Noullez, A., Bruno, R., & Bavassano, B. (2008). Heating the solar wind by a magnetohydrodynamic turbulent energy cascade. *Astrophys. J.*, *677*, L71.
- Marino, R., Sorriso-Valvo, L., Carbone, V., Veltri, P., Noullez, A., & Bruno, R. (2011). The magnetohydrodynamic turbulent cascade in the ecliptic solar wind: Study of Ulysses data. *Planetary and Space Sc.*, *59*, 592-597.
- Marino, R., Sorriso-Valvo, L., D'Amicis, R., Carbone, V., Bruno, R., & Veltri, P. (2012). On the occurrence of the third-order scaling in high latitude Solar Wind. *Astrophys. J.*, *750*, 41.
- Matthaeus, W., & Goldstein, M. (1982). Measurement of the rugged invariants of magnetohydrodynamic turbulence in the Solar Wind. *J. Geophys. Res.*, *87*, 6011-6028.
- McKeon, B. (2017). The engine behind (wall) turbulence: perspectives on scale in-

- teractions. *J. Fluid Mech.*, 817(P1).
- McWilliams, J. (2016). Submesoscale currents in the ocean. *Proc. Roy. Soc. A*, 472, 2016.0117.
- Messori, G., Caballero, R., & Faranda, D. (2017). A dynamical systems approach to studying midlatitude weather extremes. *Geophys. Res. Lett.*, 44, 1-9.
- Meyrand, R., Kiyani, K. H., & Galtier, S. (2015). Weak magnetohydrodynamic turbulence and intermittency. *J. Fluid Mech.*, 770, R1, 1-11.
- Mezić, I. (2013). Analysis of fluid flows via spectral properties of the Koopman operator. *Ann. Rev. Fluid Mech.*, 45, 357-378.
- Mininni, P., & Pouquet, A. (2009). Helicity cascades in rotating turbulence. *Phys Rev E*, 79, 026304.
- Mininni, P., Pouquet, A., & Montgomery, D. (2006). Small-scale structures in three-dimensional magnetohydrodynamic turbulence. *Phys. Rev. Lett.*, 97, 244503.
- Mininni, P., Rosenberg, D., & Pouquet, A. (2012). Isotropization at small scale of rotating helically driven turbulence. *J. Fluid Mech.*, 699, 263-279.
- Mininni, P., Rosenberg, D., Reddy, R., & Pouquet, A. (2011). A hybrid MPI-OpenMP scheme for scalable parallel pseudospectral computations for fluid turbulence. *Parallel Computing*, 37, 316-326.
- Mininni, P. D., Montgomery, D., & Pouquet, A. (2005). Numerical solutions of the three-dimensional MHD alpha model. *Phys. Rev. E*, 71, 046304.
- Mininni, P. D., & Pouquet, A. (2007). Energy spectra stemming from interactions of Alfvén waves and turbulent eddies. *Phys. Rev. Lett.*, 99, 254502.
- Moffatt, H., & Tsinober, A. (1992). Helicity in laminar and turbulent flow. *Ann. Rev. Fl. Mech.*, 24, 281-312.
- Molinari, J., & Vollaro, D. (2008). Extreme helicity and intense convective towers in hurricane Bonnie. *Month. Wea. Rev.*, 136, 4355-4372.
- Molinari, J., & Vollaro, D. (2010). Distribution of helicity, CAPE, and shear in tropical cyclones. *J. Atmos. Sci.*, 67, 274-284.
- Montgomery, D., & Turner, L. (1982). Two-and-a-half dimensional magnetohydrodynamic turbulence. *Phys Fluids*, 25, 345-349.
- Morize, C., Moisy, F., & Rabaud, M. (2005). Decaying grid-generated turbulence in a rotating tank. *Phys. Fluids*, 17(095105).
- Morrison, I., Businger, S., Marks, F., Dodge, P., & Businger, J. A. (2005). An observational case for the prevalence of roll vortices in the hurricane boundary layer. *J. Atmos. Sci.*, 62, 2662-2673.
- Müller, W., & Malapaka, S. (2013). Role of helicities for the dynamics of turbulent magnetic fields. *Geophys. Astrophys. Fluid Dyn.*, 107, 93-100.
- Newell, A., & Zakharov, V. (2008). The role of the generalized Phillips spectrum in wave turbulence. *Phys. Lett. A*, 372, 4230-4233.
- Ng, C., Rosenberg, D., Germaschewski, K., Pouquet, A., & Bhattacharjee, A. (2008). A comparison of spectral element and finite difference methods using statically refined nonconforming grids for the MHD island coalescence instability problem. *Astrophys. J. Suppl.*, 177, 613-625.
- Nore, C., Brachet, M., Politano, H., & Pouquet, A. (1997). Dynamo action in a Taylor-Green vortex near threshold. *Phys. Plasmas Lett.*, 4, 1-3.
- Oks, D., Mininni, P., Marino, R., & Pouquet, A. (2017). Inverse cascades and resonant triads in rotating and stratified turbulence. *Phys. Fluids*, 29, 111109.
- Osman, K. T., Matthaeus, W. H., Gosling, J. T., Greco, A., Servidio, S., Hnat, B., ... Phan, T. D. (2014). Magnetic reconnection and intermittent turbulence in the solar wind. *Phys. Rev. Lett.*, 112, 215002.
- Park, J. S., Shekar, A., & Graham, M. D. (2018). Bursting and critical layer frequencies in minimal turbulent dynamics and connections to exact coherent states. *Phys. Rev. Fluids*, 3(014611).
- Pathak, J., Hunt, B., Girvan, M., Lu, Z., & Ott, E. (2018). Model-free prediction of large spatiotemporally chaotic systems from data: A reservoir computing

- approach. *Phys. Rev. Lett.*, *120*, 024102.
- Perez, J. C., Mason, J., Boldyrev, S., & Cattaneo, F. (2014). Scaling properties of small-scale fluctuations in magnetohydrodynamic turbulence. *Astrophys. J. Lett.*, *793*(L13).
- Phan, T. D., Eastwood, J. P., Shay, M. A., Drake, J. F., Sonnerup, B. U. Ö., Fujimoto, M., ... Magnes, W. (2018). Electron magnetic reconnection without ion coupling in Earth's turbulent magnetosheath. *Nature*, *557*, 202-206.
- Politano, H., Carbone, V., & Pouquet, A. (1998). Determination of anomalous exponents of structure functions in two-dimensional magnetohydrodynamic turbulence. *Europhys. Lett.*, *43*, 516-521.
- Politano, H., Gomez, T., & Pouquet, A. (2003). von Kàrmàn-Howarth relationship for helical magnetohydrodynamic flows. *Phys. Rev. E*, *68*, 026315.
- Pomeau, Y. (1986). Front motion, metastability and subcritical bifurcations in hydrodynamics. *Physica D*, *23*, 3-11.
- Pomeau, Y. (2015). The transition to turbulence in parallel flows: A personal view. *Comptes Rendus Mécanique*, *343*, 210-218.
- Ponty, Y., Pouquet, A., & Sulem, P. (1995). Dynamos in weakly chaotic two-dimensional flows. *Geophys. Astrophys. Fluid Dyn.*, *79*, 239-257.
- Porter, D., Pouquet, A., & Woodward, P. (2002). Intermittency in compressible flows. *Phys. Rev. E*, *66*, 026301.
- Pouquet, A. (1993). Magnetohydrodynamic turbulence. In J. P. Zahn & J. Zinn-Justin (Eds.), *Les houches summer school on astrophysical fluid dynamics, july 1987. session xlvii* (pp. 139-227). Elsevier.
- Pouquet, A. (1996). Turbulence, statistics and structures: an introduction. In C. Chiuderi & G. Einaudi (Eds.), *v<sup>th</sup> european school in astrophysics, san miniato; lecture notes in physics "plasma astrophysics" vol. 468* (pp. 163-212). Springer-Verlag.
- Pouquet, A., Frisch, U., & Léorat, J. (1976). Strong MHD helical turbulence and the nonlinear dynamo effect. *J. Fluid Mech.*, *77*, 321-354.
- Pouquet, A., & Marino, R. (2013). Geophysical turbulence and the duality of the energy flow across scales. *Phys. Rev. Lett.*, *111*, 234501.
- Pouquet, A., Marino, R., Mininni, P. D., & Rosenberg, D. (2017). Dual constant-flux energy cascades to both large scales and small scales. *Phys. Fluids*, *29*(111108).
- Pouquet, A., Rosenberg, D., Marino, R., & Herbert, C. (2018). Scaling laws for mixing and dissipation in unforced rotating stratified turbulence. *J. Fluid Mech.*, *844*, 519-545.
- Pouquet, A., Sulem, P. L., & Meneguzzi, M. (1988). Influence of velocity-magnetic field correlations on decaying magnetohydrodynamic turbulence with neutral X-points. *Phys. Fluids*, *31*, 2635-2643.
- Pumir, A. (1996). Turbulence in homogeneous shear flows. *Phys. Fluids*, *8*, 3112-3127.
- Reddy, K. S., Kumar, R., & Verma, M. K. (2014). Anisotropic energy transfers in quasi-static magnetohydrodynamic turbulence. *Phys. Plasmas*, *21*, 102310.
- Reinken, H., Klapp, S. H. L., Bär, M., & Heidenreich, S. (2018). Derivation of a hydrodynamic theory for mesoscale dynamics in microswimmer suspensions. *Phys. Rev. E*, *97*, 022613.
- Rockström, J., Steffen, W., Noone, K., Persson, A., F. Stuart Chapin, I., Lambin, E. F., ... Foley, J. A. (2009). A safe operating space for humanity. *Nature*, *461*, 472-475.
- Rorai, C., Mininni, P., & Pouquet, A. (2014). Turbulence comes in bursts in stably stratified flows. *Phys. Rev. E*, *89*, 043002.
- Rorai, C., Rosenberg, D., Pouquet, A., & Mininni, P. (2013). Helicity dynamics in stratified turbulence in the absence of forcing. *Phys. Rev. E*, *87*, 063007.
- Rosenberg, D., Marino, R., Herbert, C., & Pouquet, A. (2016). Variations of char-



- acteristic time-scales in rotating stratified turbulence using a large parametric numerical study. *Eur. Phys. J. E*, *39*, 8.
- Rosenberg, D., Pouquet, A., Marino, R., & Mininni, P. (2015). Evidence for Bolgiano-Obukhov scaling in rotating stratified turbulence using high-resolution direct numerical simulations. *Phys. Fluids*, *27*, 055105.
- Rouet-Leduc, B., Hulbert, C., Lubbers, N., Barros, K., Humphreys, C. J., & Johnson, P. A. (2017). Machine learning predicts laboratory earthquakes. *Geophys. Res. Lett.*, *44*, 9276-9282.
- Sahoo, G., Bonaccorso, F., & Biferale, L. (2017). Discontinuous transition from direct to inverse cascade in three-dimensional turbulence. *Phys. Rev. Lett.*, *118*(164501).
- Saint-Michel, B., Herbert, E., Salort, J., Baudet, C., Bon-Mardion, M., Bonnay, P., ... Collaboration, S. (2014). Probing quantum and classical turbulence analogy through global bifurcations in a von Kàrmàn liquid Helium, nitrogen, and water experiments. *Phys. Fluids*, *26*(125109).
- Salhi, A., Baklouti, F. S., Godeferd, F., Lehner, T., & Cambon, C. (2017). Energy partition, scale by scale, in magnetic Archimedes Coriolis weak wave turbulence. *Phys. Rev. E*, *95*, 023112.
- Sano, M., & Tamai, K. (2016). A universal transition to turbulence in channel flow. *Nature Phys.*, *12*, 249-254.
- Sasaki, H., Klein, P., Qiu, B., & Sasai, Y. (2014). Impact of oceanic-scale interactions on the seasonal modulation of ocean dynamics by the atmosphere. *Nature Comm.*, *5*, 1-8.
- Saur, J., Politano, H., Pouquet, A., & Matthaeus, W. (2002). Evidence of weak MHD turbulence in the magnetosphere of Jupiter. *Astron. Astrophys.*, *386*, 699-708.
- Scott, R., & Wang, F. (2005). Direct evidence of an oceanic inverse kinetic energy cascade from satellite altimetry. *J. Phys. Oceano.*, *35*, 1650-1666.
- Servidio, S., Matthaeus, W. H., Shay, M. A., Dmitruk, P., Cassak, P. A., & Wan, M. (2010). Statistics of magnetic reconnection in two-dimensional magnetohydrodynamic turbulence. *Phys. Plasmas*, *17*, 032315.
- Seshasanayan, K., & Alexakis, A. (2016). Critical behavior in the inverse to forward energy transition in two-dimensional magnetohydrodynamic flow. *Phys. Rev. E*, *93*, 013104.
- Shebalin, J., Matthaeus, W., & Montgomery, D. (1983). Anisotropy in mhd turbulence due to a mean magnetic field. *J. Plasma Phys.*, *29*, 525-547.
- Shih, H.-Y., Hsieh, T.-L., & Goldenfeld, N. (2016). Ecological collapse and the emergence of travelling waves at the onset of shear turbulence. *Nature Phys.*, *12*, 245-248.
- Słomka, J., & Dunkel, J. (2017). Spontaneous mirror-symmetry breaking induces inverse energy cascade in 3D active fluids. *Proc. Nat. Acad. Sci.*, *114*, 2119-2124.
- Smith, C. W., Stawarz, J., Vasquez, B. J., Forman, M. A., & MacBride, B. T. (2009). Turbulent cascade at 1 AU in high cross-helicity flows. *Phys. Rev. Lett.*, *103*, 201101.
- Sorriso-Valvo, L., Marino, R., Carbone, V., Noullez, A., Lepreti, F., Veltri, P., ... Pietropaolo, E. (2007). Observation of inertial energy cascade in interplanetary space plasma. *Phys. Rev. Lett.*, *99*(115001).
- Stawarz, J., Pouquet, A., & Brachet, M.-E. (2012). Long-time properties of MHD turbulence and the role of symmetries. *Phys. Rev. E*, *86*, 036307.
- Stawarz, J., Smith, C., Vasquez, B., Forman, M., & MacBride, B. (2009). The turbulent cascade and proton heating in the Solar Wind at a AU. *Astrophys. J.*, *697*, 1119-1127.
- Stawarz, J. E., Ergun, R. E., & Goodrich, K. A. (2015). Generation of high frequency electric field activity by turbulence in the Earth's magnetotail. *J. Geo-*



- phys. Res.*, *120*, 1845-1866.
- Stawarz, J. E., & Pouquet, A. (2015). Small-scale behavior of Hall magnetohydrodynamic turbulence. *Phys. Rev. E*, *92*, 063102.
- Steenbeck, M., Krause, F., & Rädler, K.-H. (1966). Berechnung der mittleren Lorentz-feldstärke  $\overline{\mathbf{v} \times \mathbf{b}}$  für ein elektrisch leitendes medium in turbulenter, durch Coriolis-Kräfte beeinflusster bewegung. *Z. Naturforsch. A*, *21*, 369-376.
- Steffen, W., Richardson, K., Rockström, J., Cornell, S. E., Fetzer, I., Bennett, E. M., ... Sörlin, S. (2015). Planetary boundaries: Guiding human development on a changing planet. *Science*, *347*, 736-747.
- Stenzel, R., Urrutia, J., & Rousculp, C. L. (1995). Helicities of electron magnetohydrodynamic currents and fields in plasmas. *Phys Rev. Lett.*, *74*, 702-705.
- Stribling, T., & Matthaeus, W. (1990). Statistical properties of ideal three-dimensional magnetohydrodynamics. *Phys. Fluids B*, *2*, 1979-1988.
- Stribling, T., & Matthaeus, W. (1991). Relaxation processes in a low-order three-dimensional magnetohydrodynamic model. *Phys. Fluids B*, *3*, 1848-1864.
- Sujovolsky, N., & Mininni, P. (2016). Tridimensional to bidimensional transition in magnetohydrodynamic turbulence with a guide field and kinetic helicity injection. *Phys. Rev. F*, *1*, 054407.
- Tang, W., Parsons, M., Feibush, E., Choi, J., & Kurc, T. (2017). Big data machine learning for disruption predictions. In *Iaea fusion energy conference* (Vol. 26, p. 1-10).
- Taylor, J. B. (1986). Relaxation and magnetic reconnection in plasmas. *Rev. Mod. Phys.*, *58*, 741-763.
- Teitelbaum, T., & Mininni, P. (2011). The decay of turbulence in rotating flows. *Phys. Fluids*, **23**, 065105.
- Ting, A., Matthaeus, W., & Montgomery, D. (1986). Turbulence relaxation processes in magnetohydrodynamics. *Phys. Fluids*, *26*, 3261-3274.
- Tsurutani, B. T., Hajra, R., Tanimori, T., Takada, A., Bhanu, R., Mannucci, A. J., ... Gonzalez, W. D. (2016). Heliospheric plasma sheet (HPS) impingement onto the magnetosphere as a cause of relativistic electron dropouts (REDs) via coherent EMIC wave scattering with possible consequences for climate change mechanisms. *J. Geophys. Res.*, *121*, 1-27.
- Valet, J.-P., & Fournier, A. (2016). Deciphering records of geomagnetic reversals. *Rev. Geophys.*, *54*, 410-446.
- Vega, J., Murari, A., Dormido-Canto, S., Moreno, R., Pereira, A., Acero, A., & JET-EFDA Contributors. (2014). Adaptive high learning rate probabilistic disruption predictors from scratch for the next generation of tokamaks. *Nucl. Fusion*, *54*(123001).
- Veltri, P., Carbone, V., Lepreti, F., & Nigro, G. (2009). Self-organization in magnetohydrodynamic turbulence. *Encyclopedia of Complexity and System Science*, R.A. Meyers Ed., Springer.
- Verdini, A., Grappin, R., Hellinger, P., Landi, S., & Müller, W. C. (2015). Anisotropy of third-order structure functions in MHD turbulence. *Astrophys. J.*, *804*, 119.
- Waleffe, F. (1992). The nature of triad interactions in homogeneous turbulence. *Phys. Fluids*, *A4*, 350-363.
- Waleffe, F. (1997). On a self-sustaining process in shear flows. *Phys. Fluids*, *9*, 883-900.
- Wang, J.-X., Wu, J.-L., & Xiao, H. (2017). Physics-informed machine learning approach for reconstructing Reynolds-stress modeling discrepancies based on DNS data. *Phys. Rev. F*, *2*, 034603.
- Wang, P., McWilliams, J. C., & Ménesguen, C. (2014). Ageostrophic instability in rotating, stratified interior vertical shear flows. *J. Fluid Mech.*, *755*, 397-428.
- Watanabe, T., Riley, J. R., de Bruyn-Kops, S. M., Diamessis, P. J., & Zhou, Q. (2016). Turbulent/non-turbulent interfaces in wakes in stably stratified fluids.

- J. Fluid Mech.*, 797, R1.
- Wensink, H. H., Dunkel, J., Heidenreich, S., Drescher, K., Goldstein, R. E., Löwen, H., & Yeomans, J. M. (2012). Meso-scale turbulence in living fluids. *Proc. Nat. Acad. Sci.*, 109, 14308-14313.
- Wilder, F. D., Ergun, R. E., Goodrich, K. A., Goldman, M. V., Newman, D. L., Malaspina, D. M., ... Contel, O. L. (2016). Observations of whistler mode waves with nonlinear parallel electric fields near the dayside magnetic reconnection separatrix by the Magnetospheric Multiscale mission. *Geophys. Res. Lett.*, 43, 5909-5917.
- Woltjer, L. (1960). On the theory of hydromagnetic equilibrium. *Rev. Mod. Phys.*, 32, 914-915.
- Yokoi, N., & Brandenburg, A. (2016). Large-scale flow generation by inhomogeneous helicity. *Phys. Rev. E*, 93, 033125.
- Yokoi, N., & Yoshizawa, A. (1993). Statistical analysis of the effects of helicity in inhomogeneous turbulence. *Phys. Fluids*, A5, 464-477.
- Young, R. M. B., & Read, P. L. (2017). Forward and inverse kinetic energy cascades in Jupiters turbulent weather layer. *Nature Phys.*, 13, 1135-1142.
- Zhai, X., & Yeung, P. (2018). Evolution of anisotropy in direct numerical simulations of MHD turbulence in a strong magnetic field on elongated periodic domains. *Phys. Rev. F*, 3, 084602.
- Zhou, Y., Matthaeus, W., & Dmitruk, P. (2004). MHD turbulence and time scales in astrophysical and space plasmas. *Rev. Mod. Phys.*, 76, 1015-1035.
- Zhu, J.-Z., Yang, W., & Zhu, G.-Y. (2014). Purely helical absolute equilibria and chirality of (magneto)fluid turbulence. *J. Fluid Mech.*, 739, 479-501.
- Zilitinkevich, S. S., Elperin, T., Kleerorin, N., Rogachevskii, I., Esau, I., Mauritsen, T., & Miles, M. W. (2008). Turbulence energetics in stably stratified geophysical flows: Strong and weak mixing regimes. *Quart. J. Met. Roy. Soc.*, 134, 793-799.